INFOMAR DESK STUDY

PROJECT NUMBER: INF-09-25-COV

Potential of INFOMAR LiDAR reflectivity in seabed characterisation: Statistical assessment of controls and comparison with MBES backscatter

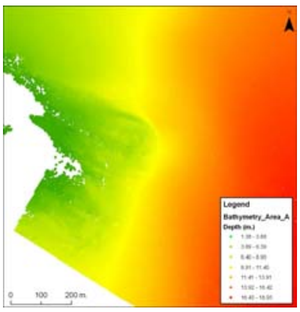

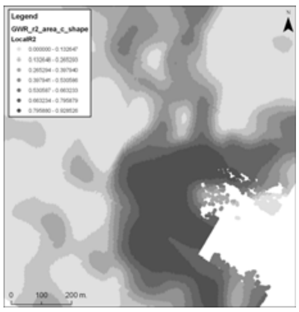

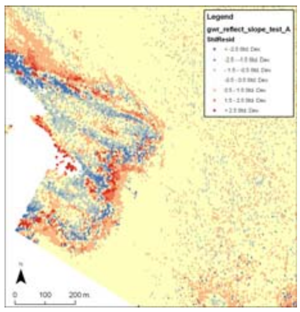

Author: Dr. Seamus Coveney

National Centre for Geocomputation

NUI Maynooth

County Kildare

Date of completion: December 2010

Table of Contents

Executive Summary

The principal aim of this study was to assess the potential for INFOMAR LiDAR reflectivity data to be used for the classification of seabed characteristics. LiDAR bathymetry has been used successfully within the INFOMAR project for the generation of bathymetric charts, and the potential for LiDAR reflectivity for seabed mapping has begun to receive scientific attention elsewhere. INFOMAR has captured a huge amount of Multi-beam Echo Sounder (MBES) sonar data, and has successfully implemented techniques to classify seabed character from MBES backscatter data. This has provided an opportunity to compare LiDAR reflectivity data with that of MBES backscatter to assess the potential of LiDAR reflectivity for seabed characterisation.

Three principal questions were addressed in this study. Firstly, the quality of the LiDAR reflectivity data was evaluated and confirmed (in section two of this report). Secondly, the statistical relationship between LiDAR reflectivity and physical variables likely to affect it were examined and quantified (in section three). A number of statistical measures were used in all these cases, to cross-check results and to examine global and local patterns in these relationships. Section four applied a similar range of statistical tests to examine the relationship between LiDAR reflectivity and MBES backscatter.

Overall, this study focused on two INFOMAR priority bays. The first bay (Blacksod Bay) was used to address the first two questions (in sections two and three), and the second bay (Galway bay) was used for the tests in section four. Blacksod bay was chosen due to the existence of two overlapping LiDAR datasets within the bay (one still due for delivery to INFOMAR from the survey contractors) and Galway bay was selected because it provided two large areas where MBES backscatter and LiDAR reflectivity coverages overlapped one another.

The findings in section two confirmed that LiDAR reflectivity values were consistent between LiDAR survey line edge-lap areas and non edge-lap areas. Section three explored the statistical relationship of LiDAR reflectivity to depth, seabed slope and LiDAR scan angle. LiDAR reflectivity was found to be strongly correlated with depth, the strongest relationship being observed in water depths of up to about 15 metres. The apparently linear relationship between reflectivity and depth at a range of depths suggested that there may be future scope to normalise LiDAR reflectivity values based upon depth. However, exploring this was beyond the scope of this study. A statistical relationship was also observed between LiDAR reflectivity and seabed slope. However, this was not as strong as the relationship observed with depth, and it was also noted that the relationship observed between reflectivity and slope was strongest in shallower water. Statistical tests applied to assess the relationship between reflectivity and LiDAR scan

angle indicated a stronger dependence of reflectivity upon scan-angle at near nadir LiDAR scan angles, but overall the statistical relationship observed was moderate.

A similar set of statistical tests was applied in section four to examine the relationship of LiDAR reflectivity and MBES backscatter. Two sub-areas were examined (one in the north of Galway bay and the other northeast of the Aran Islands). Unfortunately both these LiDAR / MBES overlap areas corresponded predominantly with water depths of 20 metres and more, so it seems highly probable that the results of analyses assessing the relationship between LiDAR reflectivity and MBES backscatter were affected by depth. Considering the strong relationship observed (in section three) between LiDAR reflectivity and depth, it seems likely that repeating the section-four tests in a shallower water area would be likely to yield substantially different results. The shallower sections of the northernmost of the two Galway bay MBES / LiDAR overlap areas did suggest a modest local statistical relationship in the shallowest areas. Therefore, it may be the case that recent LiDAR surveys conducted for INFOMAR in Blacksod bay might provide an opportunity for additional testing in the near future. Shallower water overlaps of MBES and LiDAR could be used to update this report after INFOMAR receive delivery of this new LiDAR data coverage.

In terms of additional work that might be considered in the future, research might also usefully explore the degree to which LiDAR reflectivity values can be normalised to account for depth effects. In addition, given the strong relationship between LiDAR reflectivity and water-surface returns that has been noted in other studies (Chi-Kuei & Philpot, 2007) the possibility of using simultaneously captured image data as an adjunct dataset (Costa et al. 2009) to account for these affects, and to assist in seabed characterisation might also be worth examining. In addition, reference to current limitations of the Tenix LADS LiDAR intensity algorithm (Costa et al. 2009) suggests that new data streams (Tenix LADS data were used in all aspects of this study) may also provide different results.

1. Project Background

Airborne LiDAR bathymetry (bathymetric LiDAR) data are being used within the INFOMAR project to augment bathymetry deriving from single-beam and Multi Beam Echo Sounder (MBES) surveys. The bathymetric component of the bathymetric LiDAR data are used primarily in shallow-water areas, and are combined with deeper-water sonar bathymetric surveys.

LiDAR reflectivity (backscatter) data are now being provided by most LiDAR surveyors, and reflectivity information has been provided along with the INFOMAR bathymetric LiDAR data. While the potential of MBES backscatter for seabed characterisation has already been successfully demonstrated, the degree to which bathymetric LiDAR reflectivity is still largely an open question. Some international research has been done on the subject (Chust et al. 2010, Costa et al. 2009) but the potential of bathymetric LiDAR reflectivity for seabed characterisation has yet to be unequivocally demonstrated.

The existence of overlapping INFOMAR MBES data and bathymetric LiDAR reflectivity provides a unique opportunity to assess the potential of bathymetric LiDAR reflectivity to be used for seabed characterisation. This study examines the relationship between bathymetric LiDAR reflectivity values and specific phenomena that may affect it (namely depth, seabed slope and LiDAR scan angle) before examining the relationship between MBES backscatter and bathymetric LiDAR reflectivity. If a clear relationship was to exist, this might allow routines that are routinely used to classify MBES backscatter to use bathymetric LiDAR reflectivity to classify seabed character.

The study attempts to answer the following three questions (in three separate sections) in order to draw some initial conclusions about the potential for bathymetric LiDAR reflectivity to be used to classify seabed character.

1. What is the quality of the LIDAR reflectivity data in survey line overlap and non-overlap areas?
2. To what extent are LiDAR reflectivity values modified by depth, slope and LiDAR scan angle?
3. How does LiDAR reflectivity compare with sonar backscatter (and by extension can some conclusions be drawn from this study regarding the potential for LiDAR reflectivity to be used to map seabed character?)

The first two questions are addressed using Blacksod Bay data (an area where older bathymetric LiDAR data are currently available, and for which newer bathymetric LiDAR will shortly be available). The third question is applied to MBES / LiDAR overlap areas in Galway bay.

2. LiDAR Quality evaluation

This section focuses on LADS data for Blacksod bay (figure 1). The positional accuracy of the existing INFOMAR bathymetric LiDAR data from Galway bay, Sligo bay and Tralee bay have already been externally verified with onshore ground reference data in a previous study (Coveney & Monteys, *In press*, Coveney, 2009) so the quality tests applied here focus upon bathymetric LiDAR reflectivity values only.

Successive LiDAR survey lines are typically captured in order to edge-lap preceding survey lines (in order to ensure full areal coverage, and to provide a means for comparing the georegistration of successive survey lines). The minimum, maximum, mean and standard deviation of the reflectivity values in LiDAR survey line edge-lap, and non edge-lap areas were compared in order to determine whether any significant differences could be detected.

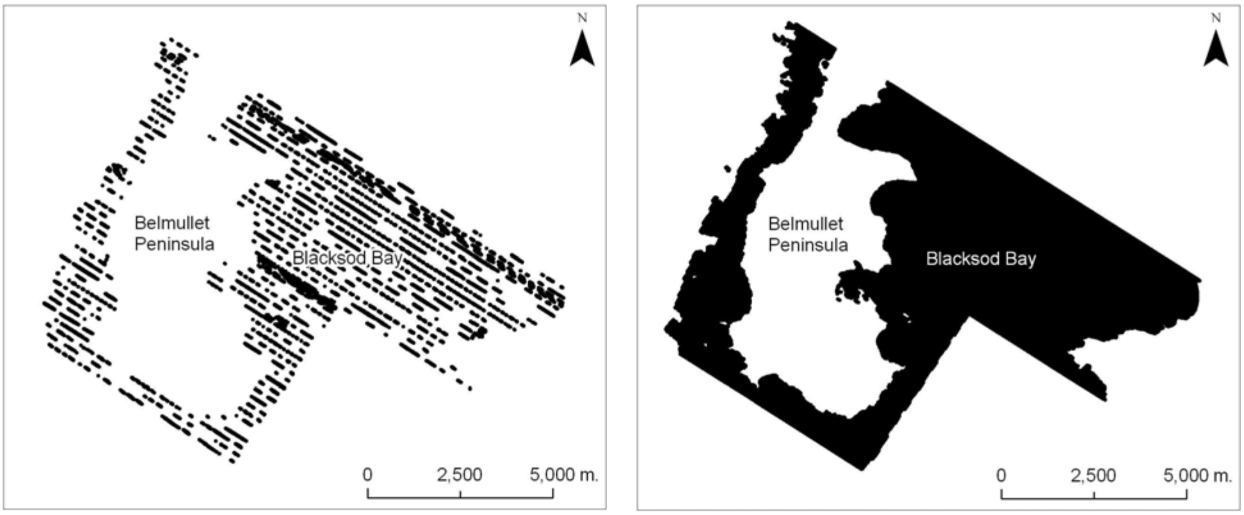

Figure 1(a) Edge-lapping LiDAR reflectivity data, (b) non edge-lapping LiDAR reflectivity data

The LiDAR reflectivity values were not calibrated against an external known radiometric source during surveying. Rather, reflectivity was defined relative to a range (presumably the full range of radiometric values in the entire dataset as opposed to within individual survey lines). It was important to consistency of reflectivity values in adjacent survey lines before embarking on a more detailed assessment of the potential for reflectivity to be used to classify seabed character.

If reflectivity measurements in successive survey lines were incorrectly registered it should have been possible to see this in colour ramp maps (figure 1). Points occurring within edge lap areas were extracted by selecting LiDAR points that had a neighbour within a 1 metre radius. Points outside of overlap areas were characterised by mean separations of 2 metres (defined by the spatial-resolution of the LiDAR survey points).

No evidence of inconsistencies between reflectivity values in edge-lap and non-edge lap areas was detected. The standard deviation and the mean of the reflectivity values occurring within edge-lap and non edge-lap areas (table 1) were also very similar, providing an additional quantitative measure of the observed consistency.

Statistical relationship tests

	Reflectivity (non edge-lap)	Reflectivity (edge-lap)
Points	2235894	60799
Minimum	1	16
Maximum	176	176
Mean	117.59	116.59
Std. Dev.	17.94	17.54

Table 1: Summary statistics of LiDAR reflectivity values for non edge-lapping points and edge-lapping survey line points.

3. Relationship of LiDAR reflectivity to depth, seabed slope and LiDAR scan angle

A series of interlinked statistical tests were applied to establish the extent to which LiDAR reflectivity returns (i.e. reflectivity that was bounced back to the LiDAR survey platform) might be influenced by LiDAR depth, seabed slope (inferred from the LiDAR depth data) and LiDAR scan-angle. These tests were applied in three (1km x 1km) sample areas that were selected (figure 2) in order to account for a wide range of water depths, seabed slopes and areas characterised by high and low spatial variation of reflectance values. These sample areas also provided three separate case study sub-areas, enabling comparisons of results. All statistical analyses were applied directly to the raw LiDAR depth and reflectivity point datasets (i.e. not rasters) in order to avoid the potential introduction of interpolation errors. Global statistical measures and local spatial statistics were applied in each sample area to examine the relationship between LiDAR reflectivity and bathymetry, seabed slope and LiDAR scan angle. The following tests were applied in each test area:

1. Scatter plot relationship visualisation
2. Pearson product moment correlation
3. Correlation P-tests
4. Ordinary Least Squares global regression
5. Spatial Autocorrelation (Moran's-Index)
6. Geographically Weighted regression

Each of these methods has its own strengths and limitations, and each successive method helped to verify and support the results of each preceding method. Methods 1 – 4 (listed above) provided global measures, and methods 5 and 6 were used to account for the possibility of local variations within each test area. Accounting for the possibility of local variation was deemed important, because if LiDAR reflectivity was found to vary in relation to depth, slope of scan-angle, some of this would be expected to be invisible within global analyses (due to averaging across the entirety of each test area).

The potential influence of depth, slope and LiDAR scan angle on the LiDAR reflectance values were examined in turn, starting with an evaluation of the relationship between depth and reflectivity within test areas A, B and C.

3.1 Reflectivity and Bathymetry

The full range of statistical tests area applied to the reflectivity data from test areas A, B and C in turn before the summary of the results are discussed at the end of sections A, B and C on the following pages.

Area A

Scatter plot relationship visualisation

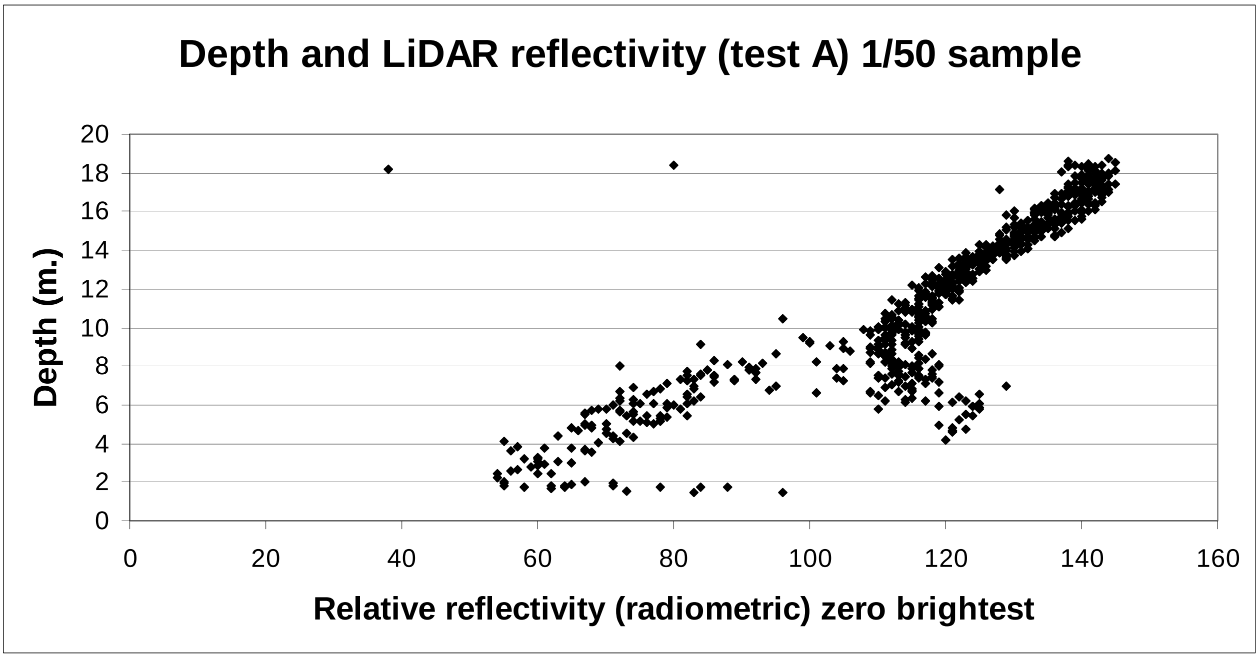

Figure 2: Scatter plot visualisation of global relationship between LiDAR reflectivity and LiDAR depth for test area 'A'.

Statistical relationship tests

Pearson product moment correlation	0.87
P-value for Pearson's correlation	<0.001
Ordinary Least Squares global regression R^2	0.78
Spatial Autocorrelation (Moran's-Index)	1.02 (highly clustered)
Likelihood clustering is a result of random chance:	<1%

Table 2: Global and local statistical test results evaluating relationship between LiDAR reflectivity and LiDAR depth for test area 'A'.

Geographically Weighted Regression

LiDAR reflectivity and depth (test area ‘A’)

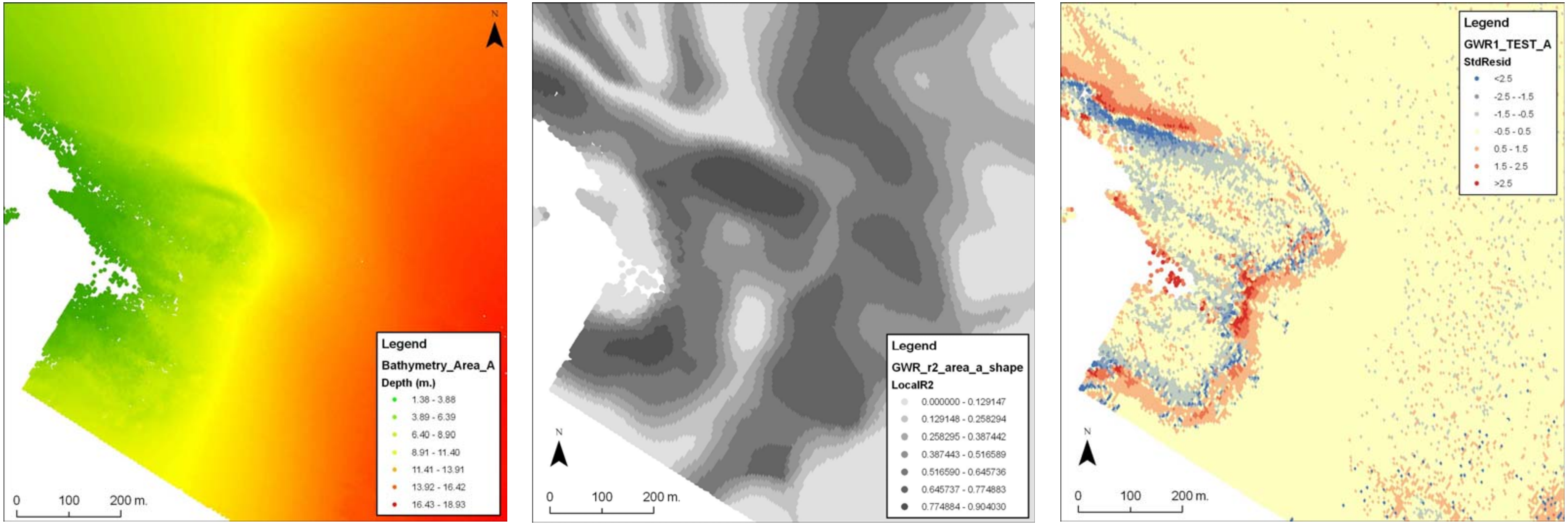

Figure 3: (a) Bathymetry area ‘A’, (b) local r2 of local GWR, and (c) local standard residual of local GWR testing applied in test area ‘A’

Area 'A' - Summary of results

All statistical tests indicated a strong relationship between LiDAR reflectivity and LiDAR-defined depth. The scatter plot (figure 2), the global correlation coefficient value of 0.87, and the global Ordinary Least Squares (OLS) regression value of 0.78 all suggested that a strong (and apparently linear) relationship existed between LiDAR reflectivity and LiDAR-defined depth (table 2). However, since global statistics tend to provide a somewhat averaged measure of a relationship occurring across the entirety of a given area, a few additional local statistics were employed to see if the observed relationships varied across test area A. The global correlation statistics were calculated in Excel and the global OLS measure was calculated in ArcGIS using the Spatial Statistics toolset.

Spatial Autocorrelation refers to the tendency for the correlation between variables to be clustered in space. Simply put this means that the degree of correlation between two variables would normally be expected to vary in different locations, based upon local variation in dependent and independent variables. The Moran's Index provides a measure of the degree to which correlation is spatially clustered within a spatial dataset. A Moran's Index spatial autocorrelation measure of 1.02 was calculated (using ArcGIS Spatial Statistics toolset) on the local residuals of the global OLS calculation. This result suggested that there was a less than 1% chance that this clustering was a result of random chance, and that strong local clustering occurred in the OLS relationship between LiDAR reflectivity and depth within test area A.

Geographically Weighted Regression (GWR) was run (using the GWR tool in the ArcGIS spatial statistics toolbox) on the local residuals of the OLS assessment (figure 3a) to explore the spatial distribution of this clustered statistical relationship. The local GWR r^2 values (r^2 values at each LiDAR point based on local regression applied to LiDAR points within a 25-metre radius of each point) and the local standard residuals at each point (figure 3c) indicated that the strongest relationships between LiDAR reflectivity and depth occurred in flat areas at depths of up to about 15 metres. Weaker relationships appeared to occur in deeper and more steeply sloping areas. Test area 'B' was characterised by flatter seabed and deeper water than test area A, so the same statistical tests were repeated in test areas B and C to verify these initial outcomes.

Area B

Scatter plot relationship visualisation

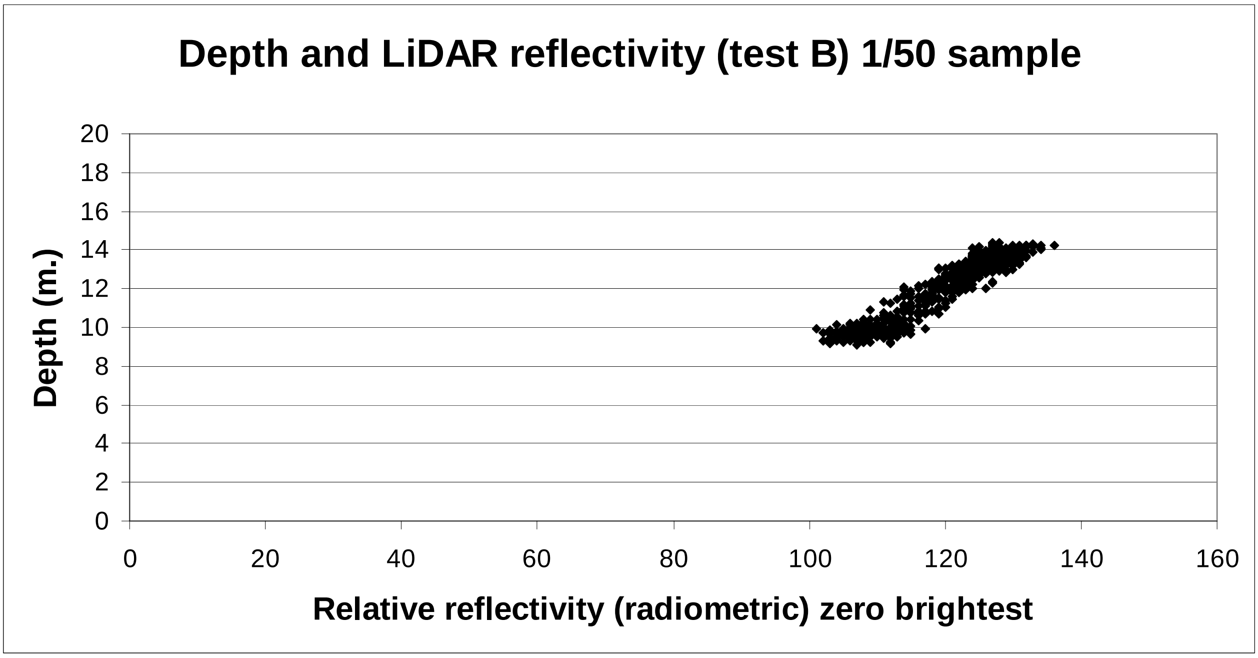

Figure 4: Scatter plot visualisation of global relationship between LiDAR reflectivity and LiDAR depth for test area 'B'.

Statistical relationship tests

Pearson product moment correlation	0.95
P-value for Pearson's correlation	<0.001
Ordinary Least Squares global regression R^2	0.91
Spatial Autocorrelation (Moran's-Index)	0.77 (highly clustered)
Likelihood clustering is a result of random chance:	<1%

Table 3: Global and local statistical test results evaluating relationship between LiDAR reflectivity and LiDAR depth for test area 'B'.

Geographically Weighted Regression

LiDAR reflectivity and depth (test area ‘B’)

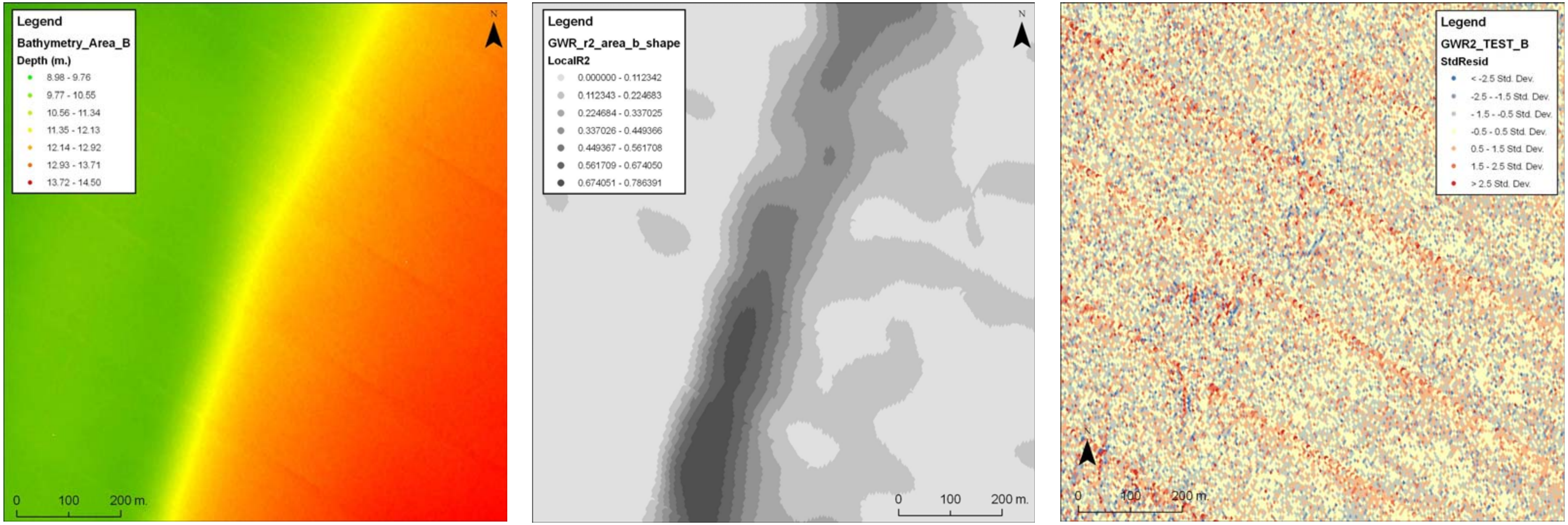

Figure 5: (a) Bathymetry area ‘B’, (b) local r2 of local GWR, and (c) local standard residual of local GWR testing applied in test area ‘B’

Area 'B' - Summary of results

The scatter plot (figure 4), the global correlation coefficient value of 0.95, and the global Ordinary Least Squares (OLS) regression value of 0.91 all again suggested that a strong (and linear) relationship existed between LiDAR reflectivity and LiDAR-defined depth (table 3).

The Moran's Index Spatial Autocorrelation measure of 0.77 indicated once again that the OLS regression residuals were spatially heterogeneous (i.e. were spatially clustered) suggesting that even stronger relationships might exist within spatially-defined clusters. However, the slightly lower Moran's-Index value for Area 'B' when taken in conjunction with the stronger correlation and OLS regression results suggested that spatial clustering of the relationship between LiDAR reflectivity and depth might be less clustered in this generally deeper water (8 – 15 metres) area. A Geographically Weighted Regression (GWR) analysis was run on the local residuals (again centred at every LiDAR point based on all points within a local 25 metre radius) of the OLS assessment (figure 5) to assess this.

The local GWR r^2 values (figure 5b) were strongly locally clustered in the centre of test area 'B' corresponding with a transition in slope at approximately 12 metres depth. Slightly weaker local GWR r^2 values occurred in areas where successive LiDAR survey lines edge-lapped one another due to the influence of close neighbour points sharing similar reflectance values. The weakest r^2 values appeared to occur at depths less than 11 metres and greater than 13 metres indicating that slope appeared to be an important influence. The spatial distribution of local standard residuals (figure 5c) suggested that the local Geographically Weighted Regression of LiDAR reflectivity and depth accounted for a significant component of the relationship between these variables in the flat seabed area represented within test area B. This (when taken with the very high global correlation and regression measures) suggested that depth accounted for a significant proportion of local variability in LiDAR reflectivity.

Area C

Scatter plot relationship visualisation

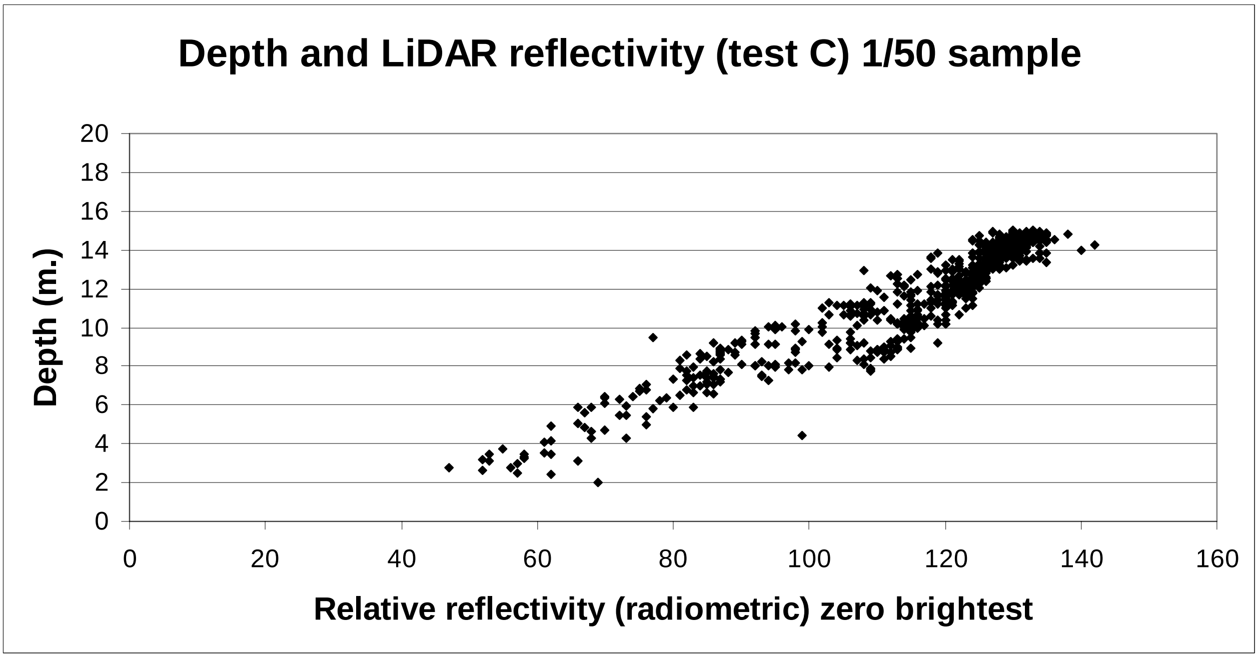

Figure 6: Scatter plot visualisation of global relationship between LiDAR reflectivity and LiDAR depth for test area 'C'.

Statistical relationship tests

Pearson product moment correlation	0.95
P-value for Pearson's correlation	<0.001
Ordinary Least Squares global regression R^2	0.89
Spatial Autocorrelation (Moran's-Index)	0.72 (highly clustered)
Likelihood clustering is a result of random chance:	<1%

Table 4: Global and local statistical test results evaluating relationship between LiDAR reflectivity and LiDAR depth for test area 'C'.

Geographically Weighted Regression

LiDAR reflectivity and depth (test area 'C')

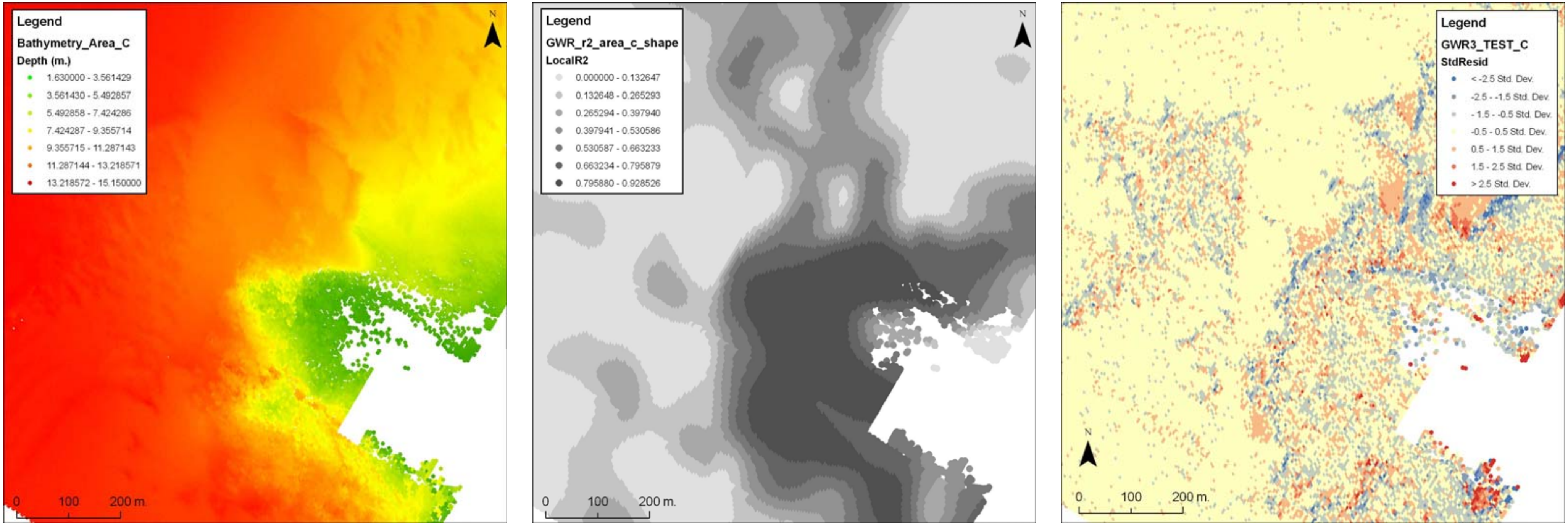

Figure 7: (a) Bathymetry area 'C', (b) local r^2 of local GWR, and (c) local standard residual of local GWR testing applied in test area 'C'

Area 'C' - Summary of results

The results here were very similar to test area A. The scatter plot (figure 6), the global correlation coefficient value of 0.95, and the global Ordinary Least Squares (OLS) regression value of 0.89 all again suggested that a very strong (and apparently linear) relationship existed between LiDAR reflectivity and LiDAR-defined depth (table 4). The Moran's Index Spatial Autocorrelation measure of 0.72 again indicated that the local OLS regression residuals were strongly spatially clustered.

The local GWR r^2 values (again based on a local 25-metre radius kernel) were again highest up to depths of 10 – 12 metres (figure 7a and 7b). Variability in the standard residuals map (an indicator of where local regression appears to be a less convincing indicator of the relationship between LiDAR reflectivity and depth) again suggest (figure 7c) that the relationship between LiDAR reflectivity and depth is strongest in flat areas. The degree to which the single-returns LIDAR reflectivity data values were related to seabed slope was examined in detail in section 3.2.

3.2 *Reflectivity and Slope*

Area A

Scatter plot relationship visualisation

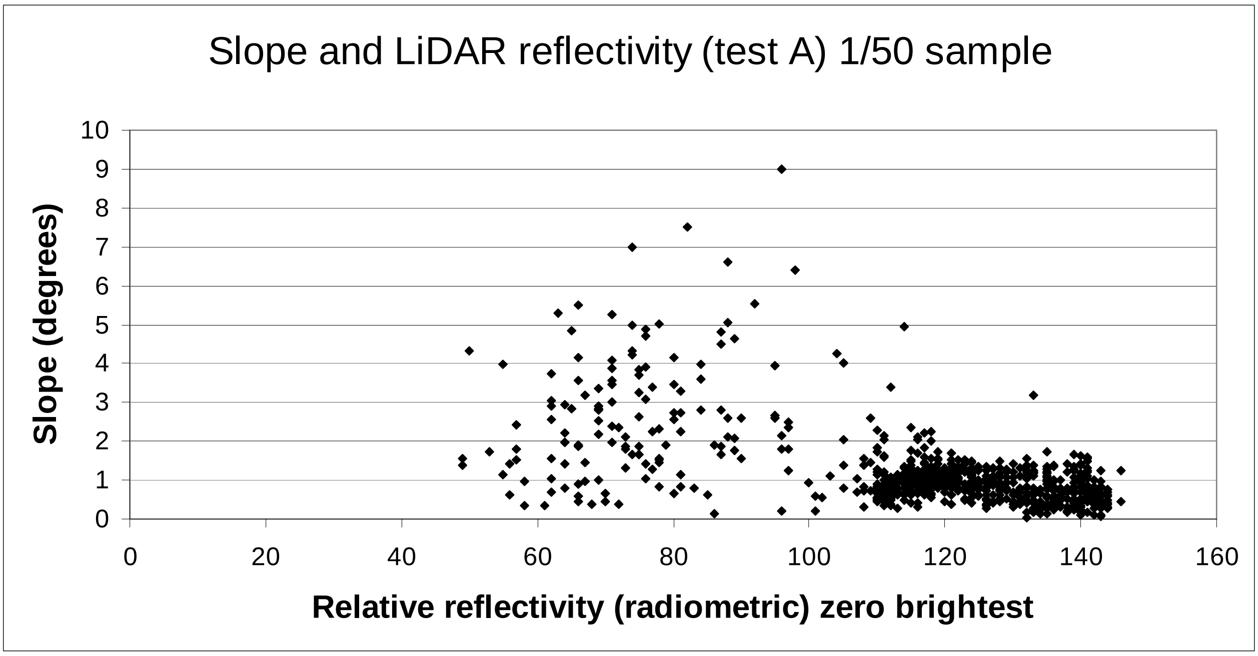

Figure 8: Scatter plot visualisation of global relationship between LiDAR reflectivity and LiDAR-derived slope depth for test area 'A'.

Statistical relationship tests

Pearson product moment correlation	-0.57
P-value for Pearson's correlation	<0.001
Ordinary Least Squares global regression R^2	0.0003
Spatial Autocorrelation (Moran's-Index)	0.77 (highly clustered)
Likelihood clustering is a result of random chance:	<1%

Table 5: Global and local statistical test results evaluating relationship between LiDAR reflectivity and LiDAR depth for test area 'C'.

Geographically Weighted Regression

LiDAR reflectivity and slope (test area 'A')

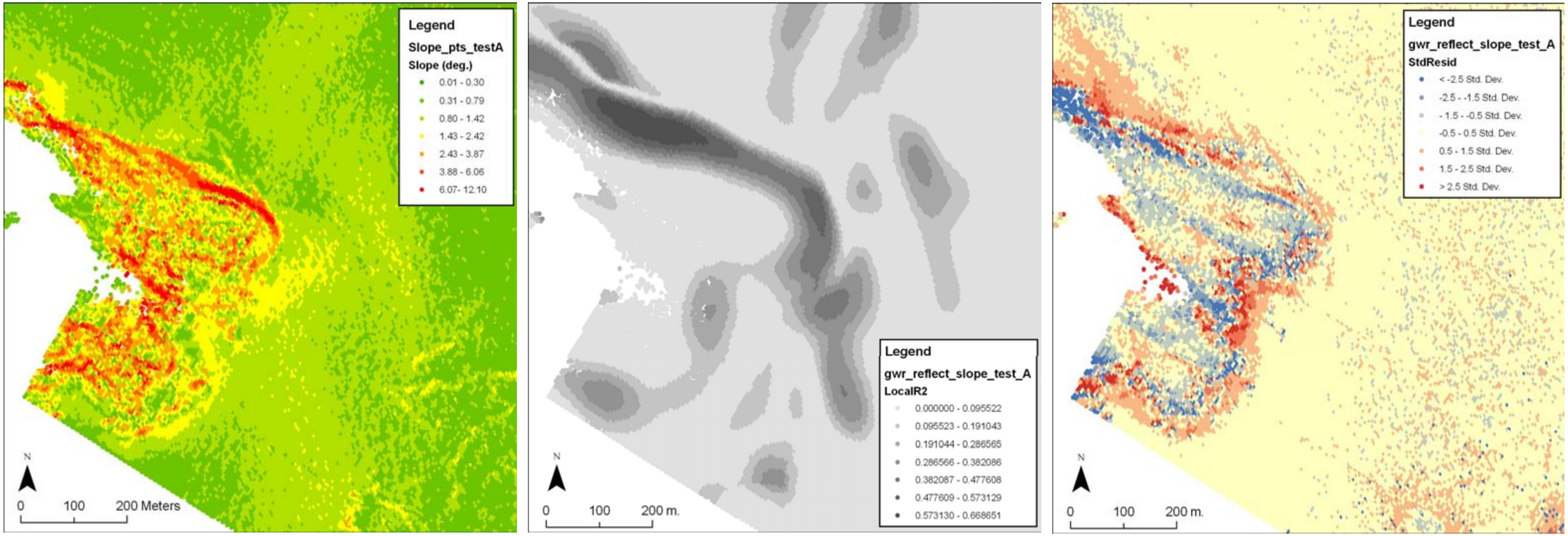

Figure 9: (a) Slope area 'A', (b) local r^2 of local GWR, and (c) local standard residual of local GWR testing applied in test area 'A'

Area 'A' - Summary of results

The scatter plot (figure 8), the global correlation coefficient value of -0.57 indicated a moderate tendency for LiDAR reflectivity to decrease as seabed slope increases, but the global Ordinary Least Squares (OLS) regression value of 0.0003 suggested that this was weak (table 5). It should be noted however that the brightest LiDAR reflectivity values (those values closest to zero) were all associated with moderate slopes (under 5 degrees). Closer examination of the slope map (figure 9a) indicates that theses steeper sloped areas (very few points were characterised by slopes over 6 degrees) were all in shallow water. Therefore, it was possible that the correlation result of -0.57 (table 5) may have been related more to depth than to slope. The OLS regression result suggested that this may indeed have been the case, but further examination was required before any conclusions could be drawn.

The Moran's Index Spatial Autocorrelation measure of 0.77 indicated that the OLS regression residuals were strongly spatially clustered, so a GWR analysis was run to examine determine the areas where LiDAR reflectivity and slope displayed the strongest relationships. The local GWR r^2 values (figure 9b) were notably strongest outside of the shallower areas where the slope was steepest and were strongest in the (still relatively shallow water) are fringing the more steeply sloped shallows (figure 9a). Local GWR r^2 values tended to reduce in water deeper than about 12 metres, with a few local GWR r^2 'peaks' in evidence in the flattest areas at depths up to approximately 15 metres. The spatial distribution of negative GWR local standard residuals in association with the sloped areas and positive local standard residuals with shall-water flat areas (figure 9c) also supported the theory that moderate slope affected reduced LiDAR reflectivity in shallow water. All the results tended also to suggest that depth accounted for a much more significant proportion of local variability in LiDAR reflectivity than slope. The same suite of tests was applied in test areas A and B to verify these initial results.

Area B
Scatter plot relationship visualisation

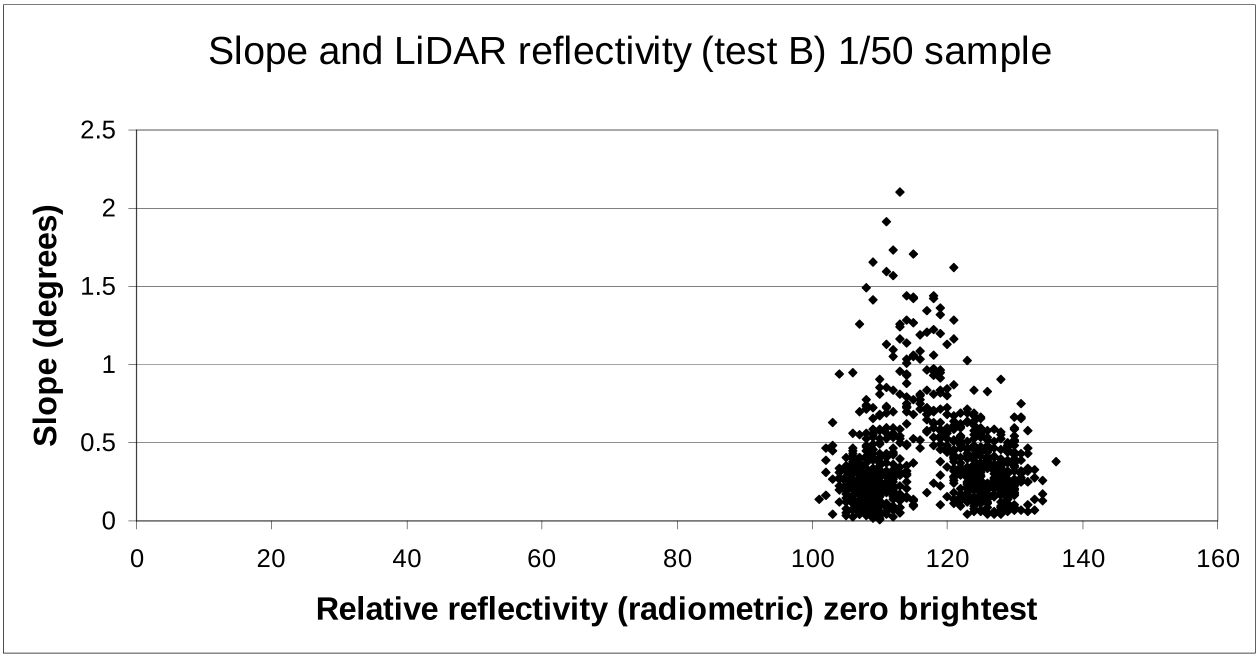

Figure 10: Scatter plot visualisation of global relationship between LiDAR reflectivity and LiDAR-derived slope depth for test area ‘B’.

Statistical relationship tests

Pearson product moment correlation	0.01
P-value for Pearson’s correlation	<0.001
Ordinary Least Squares global regression R^2	0.00002
Spatial Autocorrelation (Moran’s-Index)	0.89 (highly clustered)
Likelihood clustering is a result of random chance:	<1%

Table 6: Global and local statistical test results evaluating relationship between LiDAR reflectivity and LiDAR depth for test area ‘C’.

Geographically Weighted Regression

LiDAR reflectivity and slope (test area 'B')

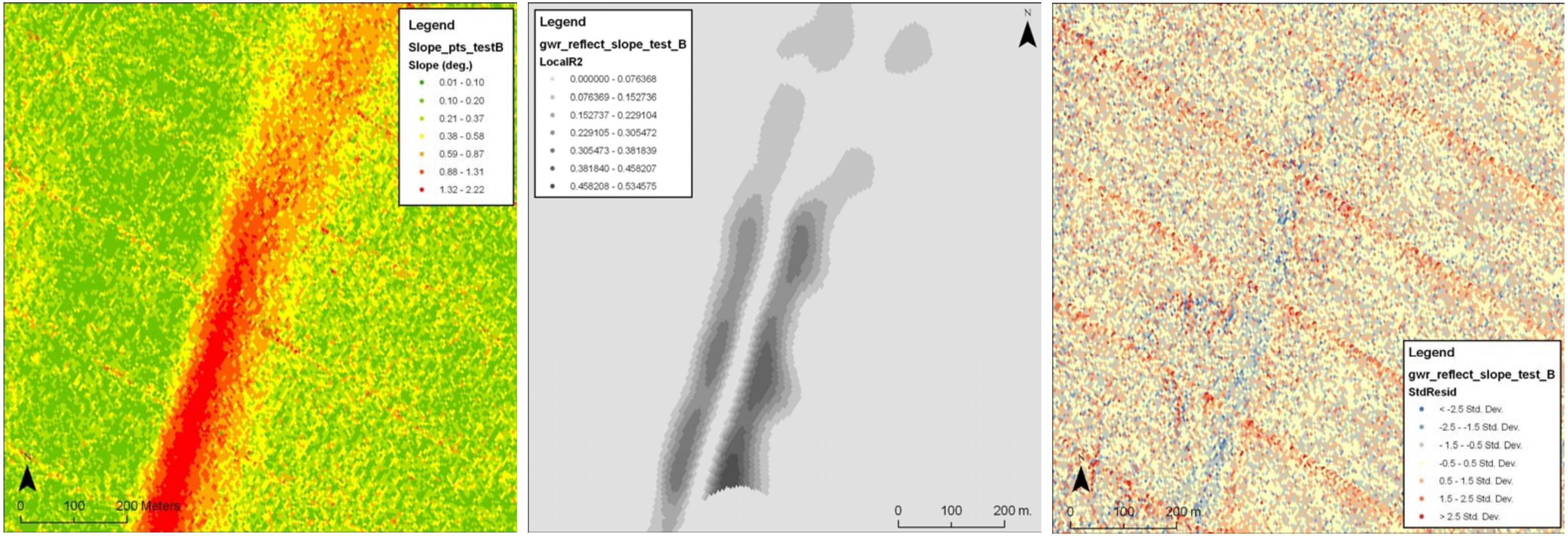

Figure 11: (a) Slope area 'B', (b) local r^2 of local GWR, and (c) local standard residual of local GWR testing applied in test area 'B'

Area ‘B’ - Summary of results

The scatter plot (figure 10), the global correlation coefficient value of 0.01 and the global Ordinary Least Squares (OLS) regression value of 0.00002 (table 6) suggested that LiDAR reflectivity was not related to slope in the depth range between 10 and 15 metres. However, the global Moran’s Index of 0.89 indicated that the OLS regression residuals were strongly spatially clustered, so a GWR analysis was run to examine determine the areas where LiDAR reflectivity and slope displayed the strongest relationships.

The strongest GWR r^2 values (of approximately 0.5) displayed a strong association with a linear feature in test area ‘B’ (figure 11b). This linear feature appears to represent a slope discontinuity (figure 11a) in the middle of test area B. A double linear phenomenon apparent in the local GWR r^2 map (figure 11b) appeared to suggest the presence of an artificial feature (perhaps a pipe or underwater cable route). However, the most important conclusion to be drawn in this instance was that even very subtle changes in slope at depths of about 12 metres appeared to affect LiDAR reflectivity. A vague impression of a double linear phenomenon corresponding to a double negative standard residual cluster in this region appears to confirm this theory.

Area C

Scatter plot relationship visualisation

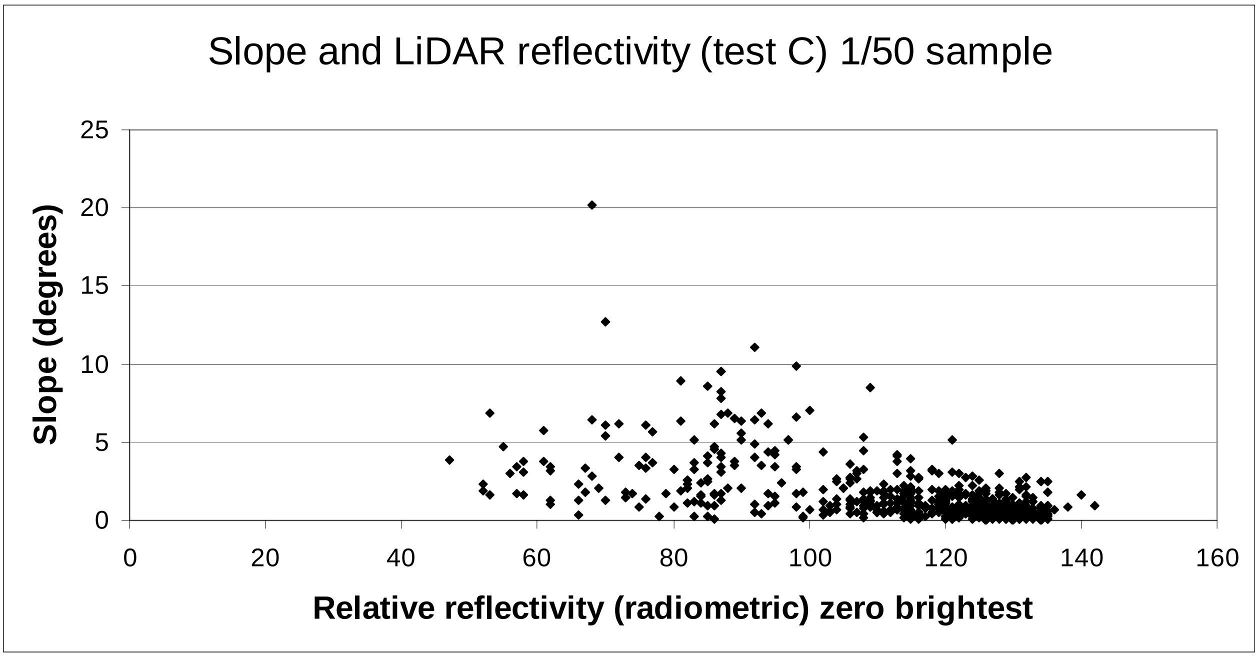

Figure 12: Scatter plot visualisation of global relationship between LiDAR reflectivity and LiDAR-derived slope depth for test area 'C'.

Statistical relationship tests

Pearson product moment correlation	-0.58
P-value for Pearson's correlation	<0.001
Ordinary Least Squares global regression R^2	0.0001
Spatial Autocorrelation (Moran's-Index)	0.96 (highly clustered)
Likelihood clustering is a result of random chance:	<1%

Table 7: Global and local statistical test results evaluating relationship between LiDAR reflectivity and LiDAR depth for test area 'C'.

Geographically Weighted Regression

LiDAR reflectivity and slope (test area 'C')

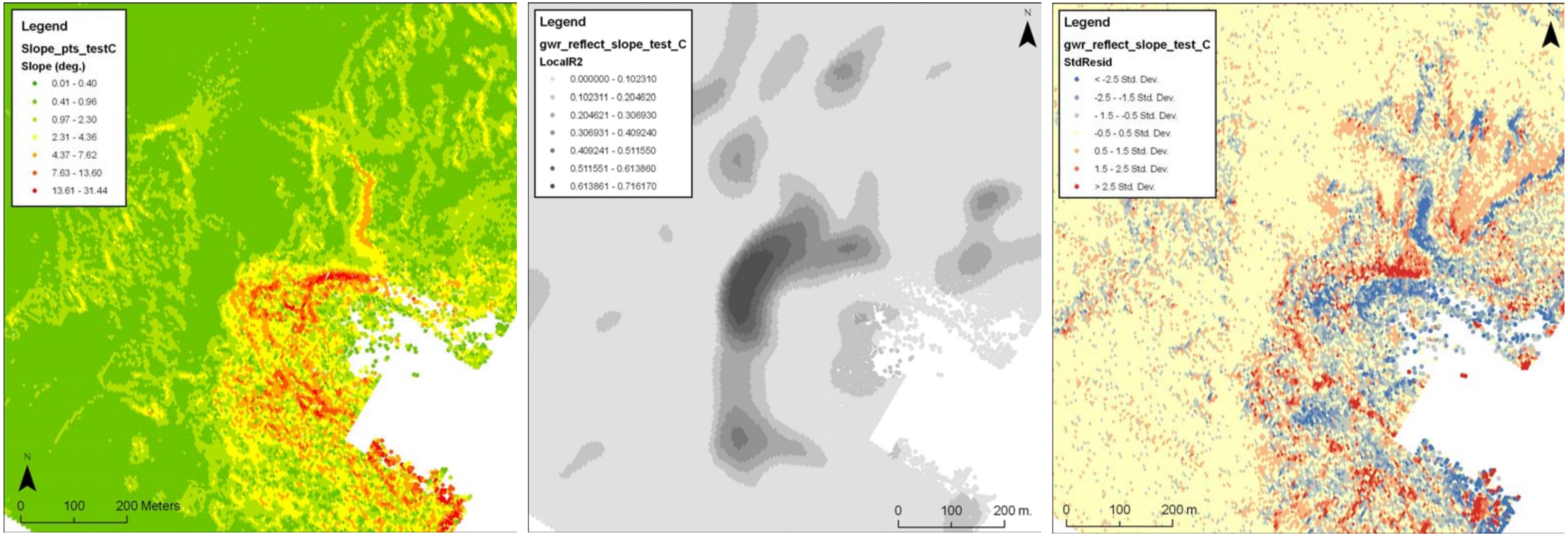

Figure 13: (a) Slope area 'C', (b) local r^2 of local GWR, and (c) local standard residual of local GWR testing applied in test area 'C'

Area 'C' - Summary of results

Similar to the case in test area A, the scatter plot (figure 12) for test area 'C' and the global correlation coefficient value of -0.58 initially suggested a moderate tendency for LiDAR reflectivity to decrease as seabed slope increases. However, the global Ordinary Least Squares (OLS) regression value of 0.0001 yet again suggested that this may be too simplistic (table 7).

The Moran's Index Spatial Autocorrelation measure of 0.96 again indicated that the OLS regression residuals were strongly spatially clustered. The local GWR r^2 values (figure 13b) were strongest in flat areas fringing the more steeply sloped shallows (figure 13a). Once again local GWR r^2 values tended to reduce in water deeper than about 12 metres, with a few local GWR r^2 'peaks' in flat areas at depths up about 13 or 14 metres. The spatial distribution of negative GWR local standard residuals in association with the sloped areas and positive local standard residuals with shall-water flat areas (figure 13c) also supported the observation that moderate slope affected reduced LiDAR reflectivity in shallow water.

Quantification of the proportional contributions of depth and slope to LiDAR reflectivity was outside of the scope of this study, but the results did suggest that depth accounted for a much more significant proportion of local variability in LiDAR reflectivity than could be attributed to slope.

3.3 Reflectivity and LiDAR scan angle

Area A

Scatter plot relationship visualisation

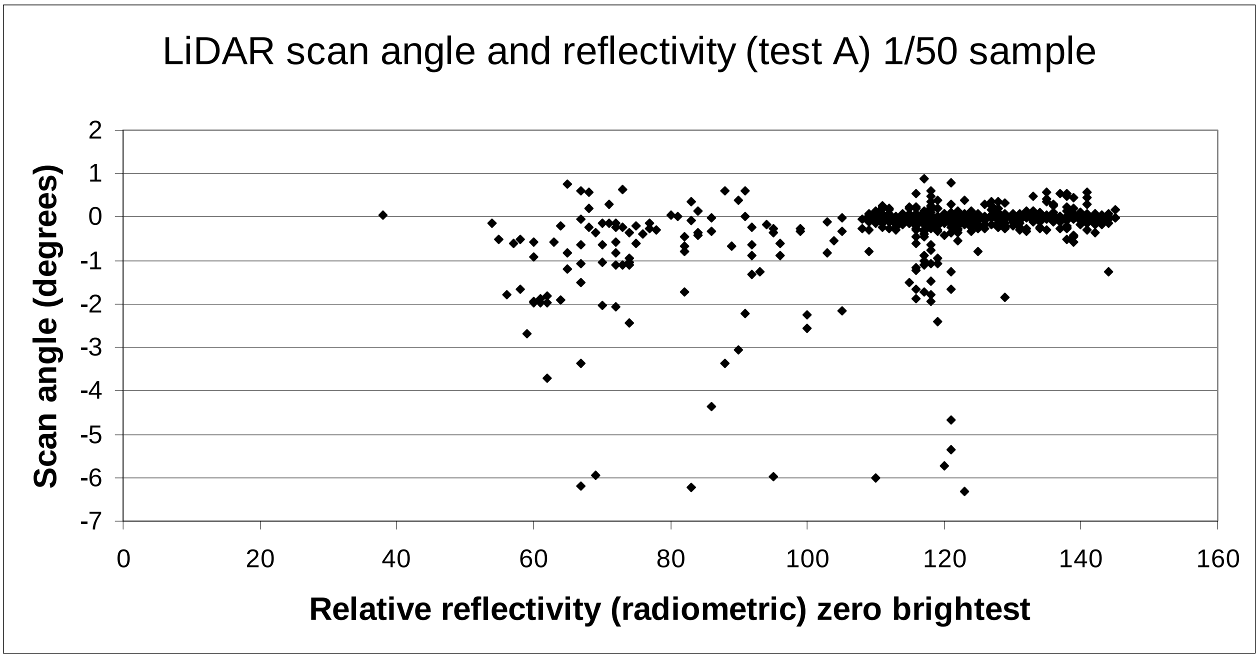

Figure 14: Scatter plot visualisation of global relationship between LiDAR reflectivity and LiDAR side scan-angle for test area 'A'.

Statistical relationship tests

Pearson product moment correlation	0.37
P-value for Pearson's correlation	<0.001
Ordinary Least Squares global regression R^2	0.005
Spatial Autocorrelation (Moran's-Index)	0.77 (highly clustered)
Likelihood clustering is a result of random chance:	<1%

Table 8: Global and local statistical test results evaluating relationship between LiDAR reflectivity and LiDAR side scan-angle for test area 'A'.

Geographically Weighted Regression

LiDAR reflectivity and LiDAR side scan-angle (test area ‘A’)

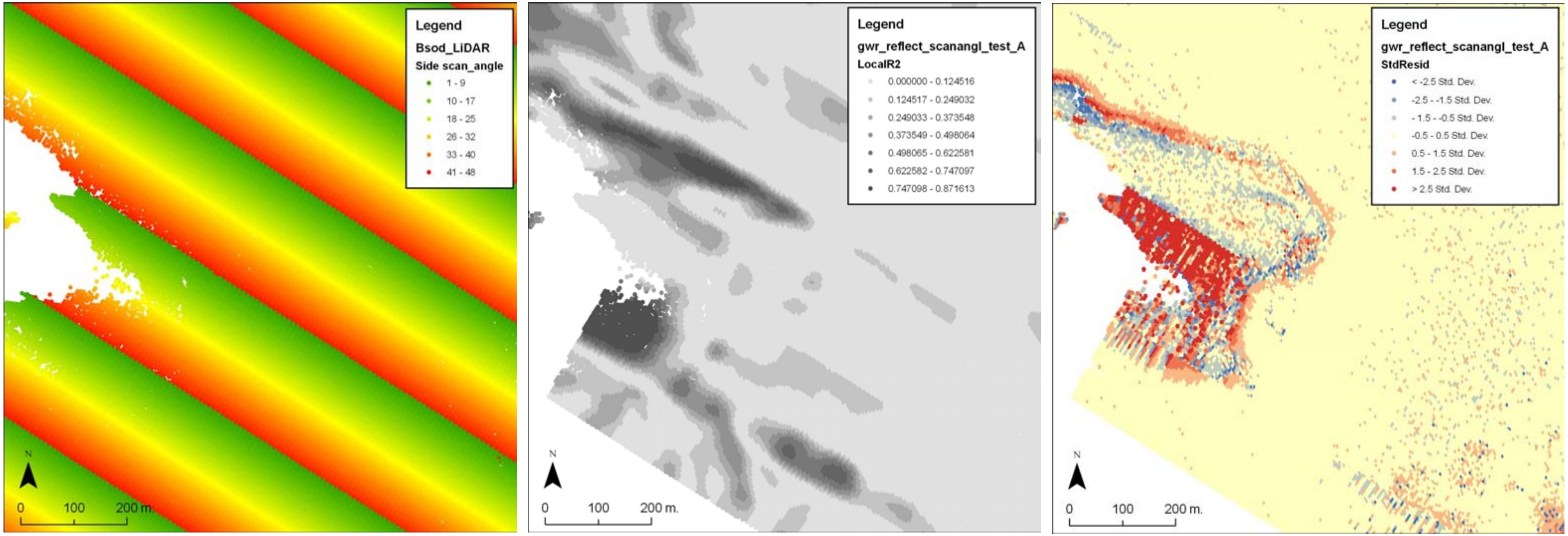

Figure 15: (a) LiDAR side scan-angle area ‘A’, (b) local r^2 of local GWR, and (c) local standard residual of local GWR testing applied in test area ‘A’

Area ‘A’ - Summary of results

The scatter plot (figure 14) for test area ‘A’ and the global correlation coefficient value of 0.37 appeared unpromising and the global Ordinary Least Squares (OLS) regression value of 0.005 seemed to further confirm this (table 8). However, as was the case in previous analyses, the Moran’s-Index value of 0.77 highlighted strong clustering in the local OLS residuals. The GWR analysis identified the nature of this clustering (figure 15b) demonstrating the association of the higher GWR r^2 values with the shallower LiDAR scan-angles. Once again the local clusters evident in the GWR standard residuals map (figure 15c) highlighted a stronger relationship between LIDAR reflectivity and an indicator variable (scan-angle in this case) in shallower water.

Test B

Scatter plot relationship visualisation

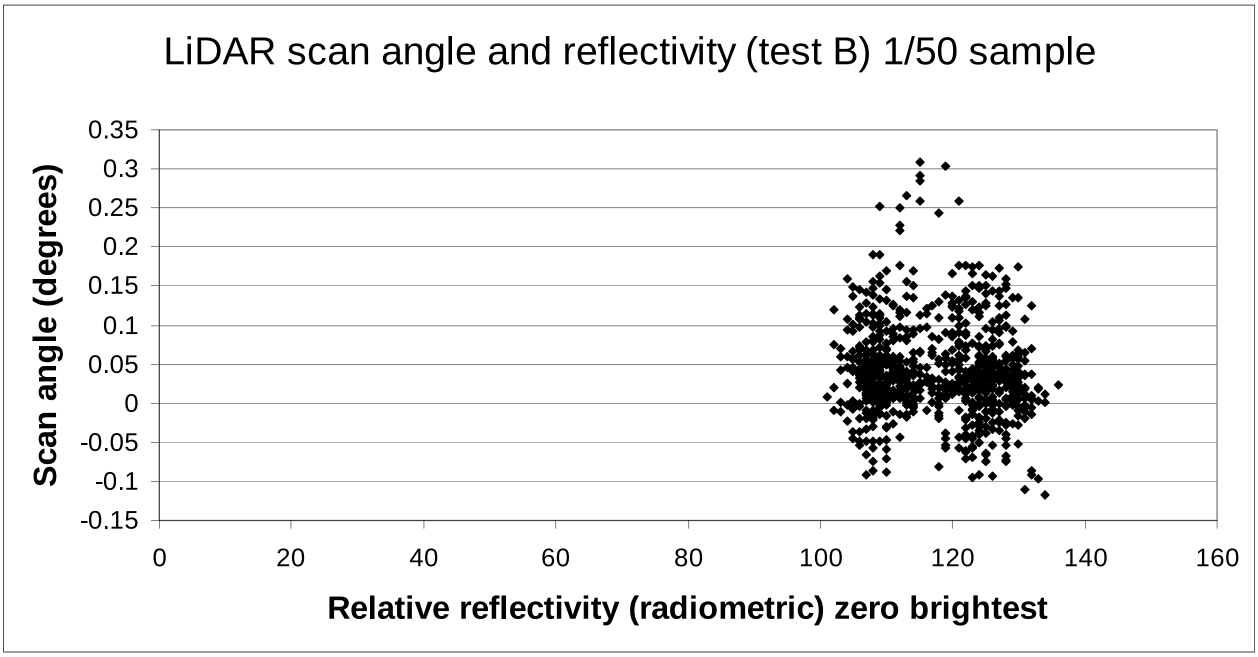

Figure 16: Scatter plot visualisation of global relationship between LiDAR reflectivity and LiDAR side scan-angle for test area 'B'.

Statistical relationship tests

Pearson product moment correlation	-0.11
P-value for Pearson's correlation	<0.001
Ordinary Least Squares global regression R^2	0.002
Spatial Autocorrelation (Moran's-Index)	0.90 (highly clustered)
Likelihood clustering is a result of random chance:	<1%

Table 9: Global and local statistical test results evaluating relationship between LiDAR reflectivity and LiDAR side scan-angle for test area 'B'

Geographically Weighted Regression

LiDAR reflectivity and LiDAR side scan-angle (test area 'B')

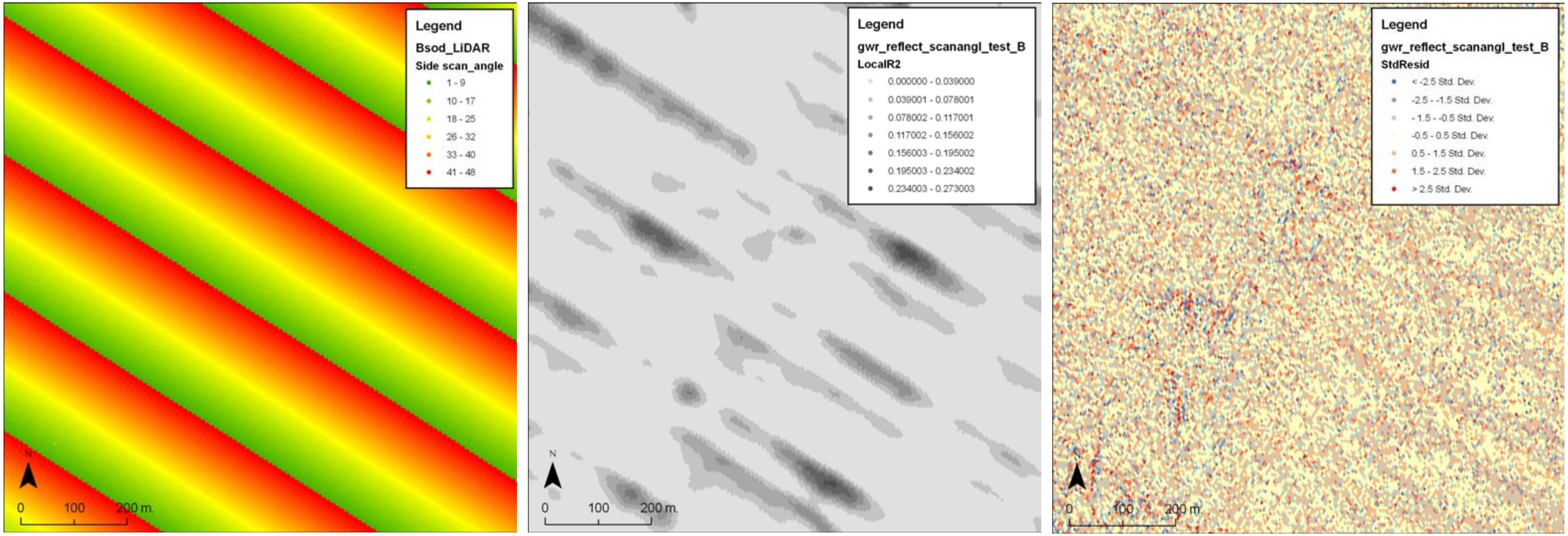

Figure 17: (a) LiDAR side scan-angle area 'B', (b) local r^2 of local GWR, and (c) local standard residual of local GWR testing applied in test area 'B'

Area ‘B’ - Summary of results

The results here were very similar to test area A. The scatter plot (figure 16), the global correlation coefficient value of -0.11 and the global Ordinary Least Squares (OLS) regression value of 0.002 all indicated a weak relationship between LiDAR reflectivity and LiDAR scan-angle (table 9). The Moran’s-Index value of 0.90 highlighted strong clustering in the local OLS residuals and the GWR analysis pinpointed the locations of these clusters (figure 17b). Modest GWR r^2 value clusters once more coincided with shallower LiDAR scan-angles. However, the water depth in test area ‘B’ appears to have been too deep to result in any depth-related pattern in the GWR standard residuals map (figure 17c).

Area C

Scatter plot relationship visualisation

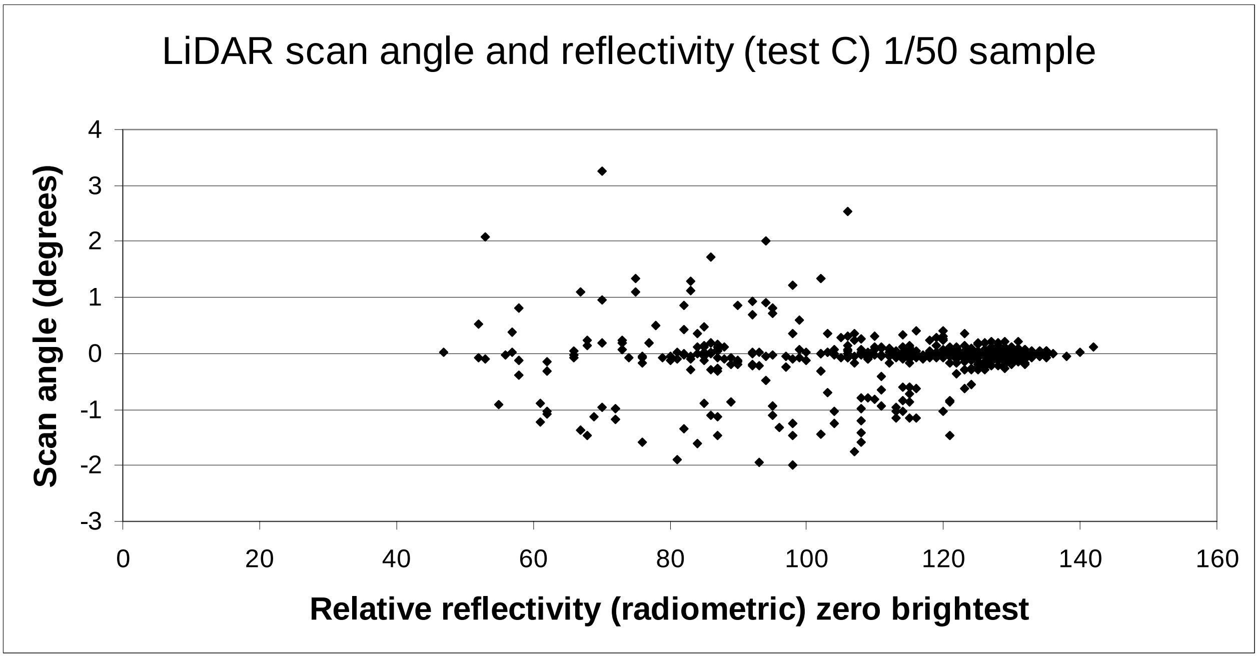

Figure 18: Scatter plot visualisation of global relationship between LiDAR reflectivity and LiDAR side scan-angle for test area 'C'.

Statistical relationship tests

Pearson product moment correlation	0.06
P-value for Pearson's correlation	<0.001
Ordinary Least Squares global regression R^2	0.002
Spatial Autocorrelation (Moran's-Index)	0.99 (highly clustered)
Likelihood clustering is a result of random chance:	<1%

Table 10: Global and local statistical test results evaluating relationship between LiDAR reflectivity and LiDAR side scan-angle for test area 'C'

Geographically Weighted Regression

LiDAR reflectivity and LiDAR side scan-angle (test area ‘C’)

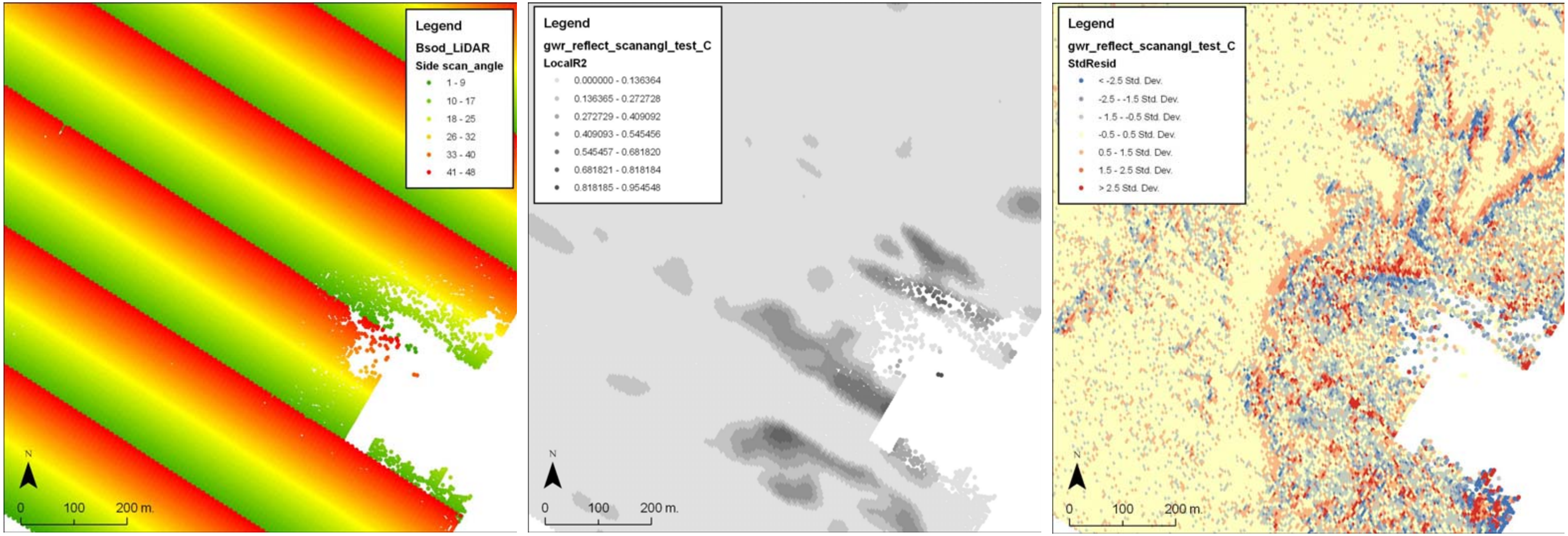

Figure 19: (a) LiDAR side scan-angle area ‘C’, (b) local r^2 of local GWR, and (c) local standard residual of local GWR testing applied in test area ‘C’

Area 'C' - Summary of results

The results here were very similar to test areas A and B. The scatter plot (figure 18), the global correlation coefficient value of 0.06 and the global Ordinary Least Squares (OLS) regression value of 0.002 all indicated a weak relationship between LiDAR reflectivity and LiDAR scan-angle (table 10). The Moran's-Index value of 0.99 highlighted strong clustering in the local OLS residuals and the GWR analysis pinpointed the locations of these clusters (figure 19b). Strong GWR r^2 value clusters once more coincided with shallower LiDAR scan-angles. The local GWR r^2 clusters also highlighted a stronger relationship between LIDAR reflectivity and LiDAR scan-angle in shallower water.

Section 4: Relationship between LiDAR reflectivity and MBES sonar backscatter

This section of the study focused on Galway bay, applying statistical analysis to the two large LiDAR / MBES overlap areas that exist within the bay (figure 20). Similar to section three, a series of successive statistical tests were applied in order to assess the nature of the global and local relationships between LiDAR reflectivity and sonar backscatter. Once again, analysis was applied to point datasets (rather than rasters) in order to avoid errors due to interpolation. The LiDAR and sonar point data were integrated for the analysis. The mean resolution of the LiDAR points was 2-metres and the mean resolution of the sonar points was <1 metre, so the MBES and LiDAR points were not exactly spatially coincident. The MBES attribute data were joined to the LiDAR data by selecting the closest MBES point (within a maximum radius of 1m) to each LiDAR point. This reduced the size of the MBES dataset in each overlap area (from >3 million points) and ensured that comparisons were applied only on cases where MBES points lay close to the LiDAR points. The MBES backscatter values ranged from -40 (lowest reflectance) to 0 (highest reflectance) so 41 was added to all MBES values to bring them into a positive range prior to statistical comparison with the positive LiDAR reflectivity values. Statistical comparisons were applied to optimal MBES beam numbers (defined by INFOMAR) 30, 40, 70 & 80 for each of the two survey areas.

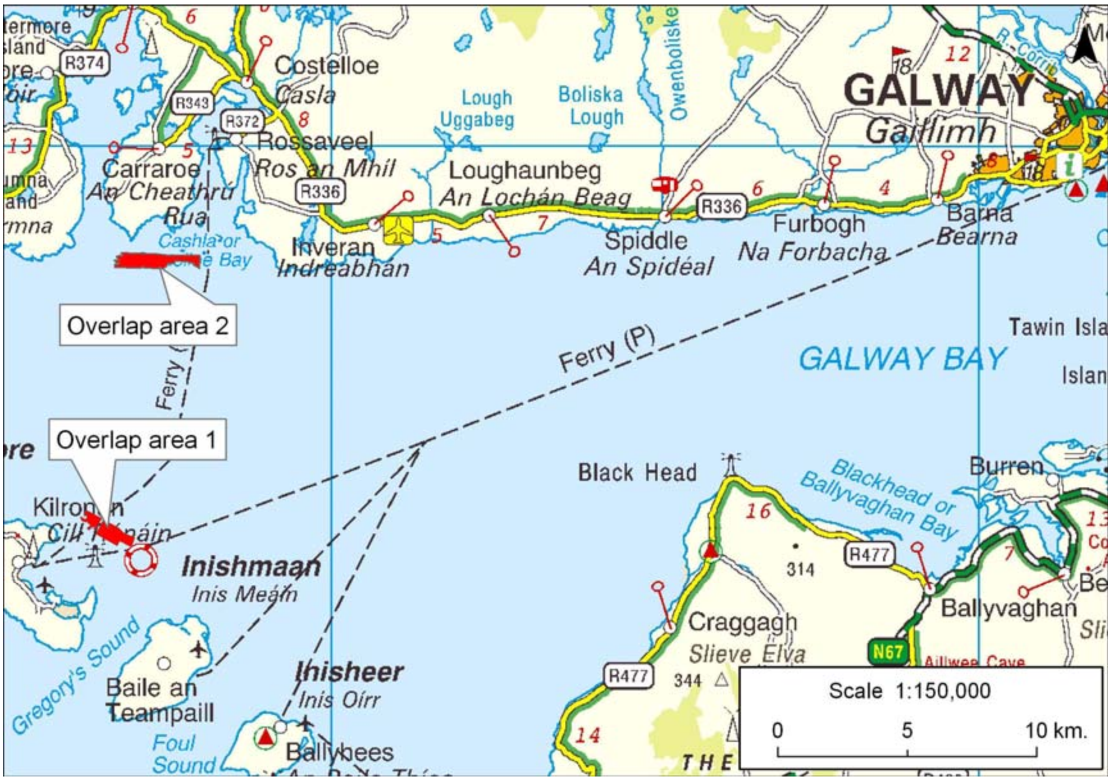

Figure 20: Galway bay MBES / LiDAR overlap areas

MBES LiDAR overlap analysis

Overlap area 1 Scatter plot relationship visualisation

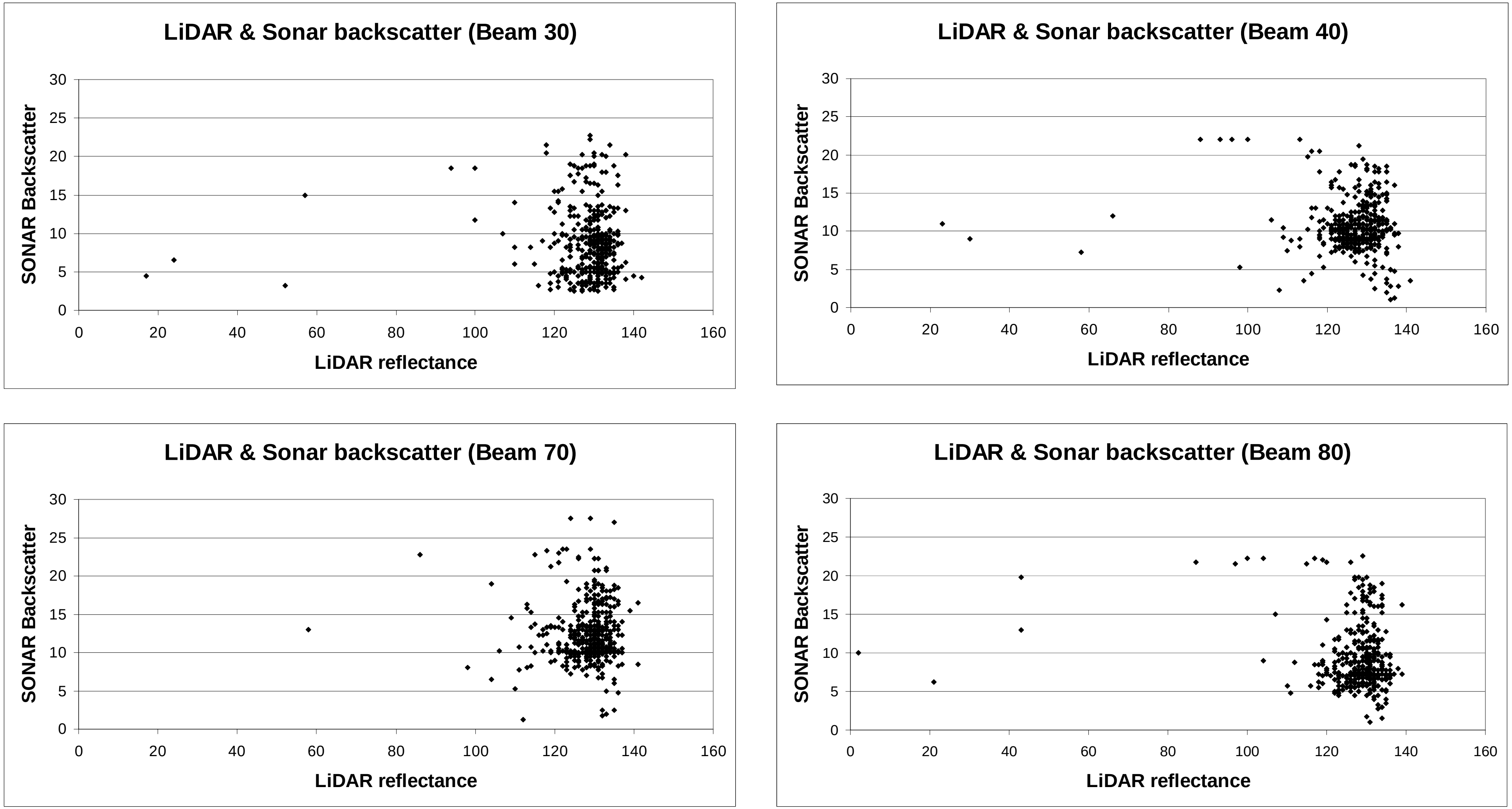

Figure 21: Scatter plot visualisation of global relationship between LiDAR reflectivity and MBES backscatter (for MBES beam numbers 30, 40, 70 and 80) for LiDAR MBES overlap area 1.

Statistical relationship tests

	Beam 30	Beam 40	Beam 70	Beam 80
Pearson's Correlation	-0.017	-0.07	-0.02	-0.14
Pearson's p-test	<0.001	<0.001	<0.001	<0.001
OLS regression	*0.0002			
Moran's Index	*0.038			
Likelihood Moran's-I result of random chance	<1%			

Table 11: Global and local statistical test results evaluating relationship between LiDAR reflectivity and MBES backscatter (for MBES beam numbers 30, 40, 70 and 80) for LiDAR MBES overlap area 1. *Note – OLS and Moran's-I tests applied to entire overlap area 1.

Geographically Weighted Regression

Overlap area 1

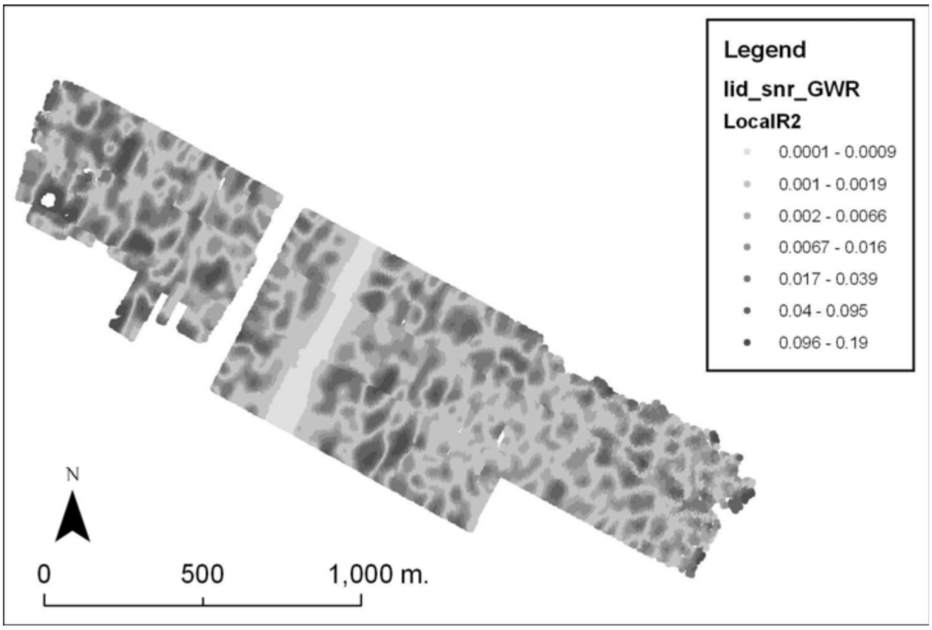

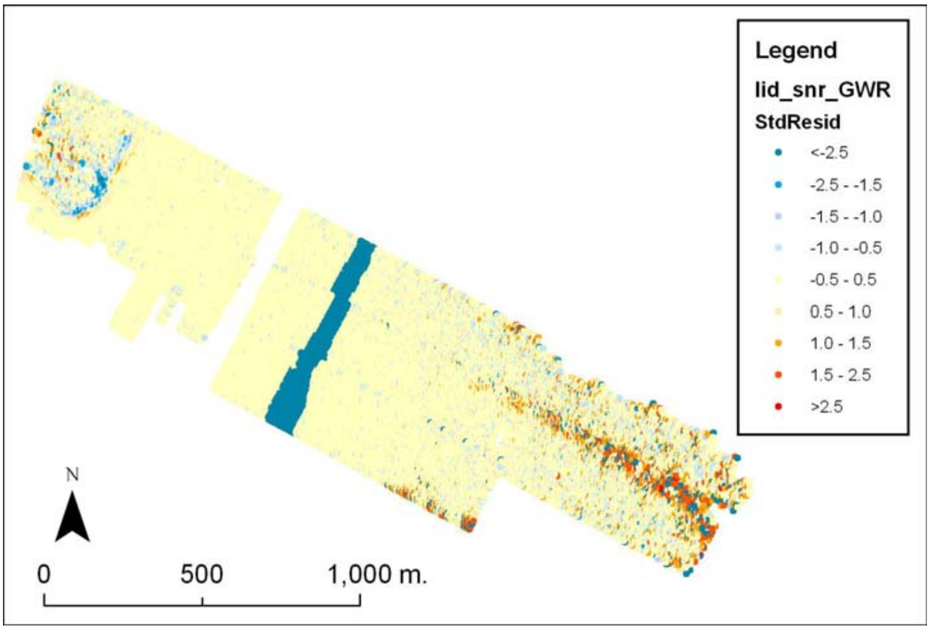

Figure 22: (a) local r^2 of local GWR, and (b) local standard residual of local GWR testing applied in Overlap area 1.

Overlap area 1: Summary of results

The scatter plots (figure 21) Pearson's correlation and OLS regression results (table 11) all suggested a weak relationship between LiDAR reflectivity and MBES backscatter. However, it should be noted that both overlap areas 1 and 2 (figure 20) were both in water depths of greater than 15 metres. Given the findings in section three, it is possible that the available LiDAR / MBES overlap areas were a little too deep to expect a strong correlation to be observed across the entirety of overlap area 1.

The Moran's-Index value of 0.038 (table 11) suggested that a clustered pattern may be present, and the GWR provided a clearer picture of the nature of this clustering. The GWR local r2 values were low (figure 22a) and the GWR local standard residuals were very subtle also (figure 22a), making it difficult to attribute the spatial patterns noted to a convincing relationship between LiDAR reflectivity and MBES backscatter. Overlap area 2 was examined using similar methods to assess

Overlap area 2

Scatter plot relationship visualisation

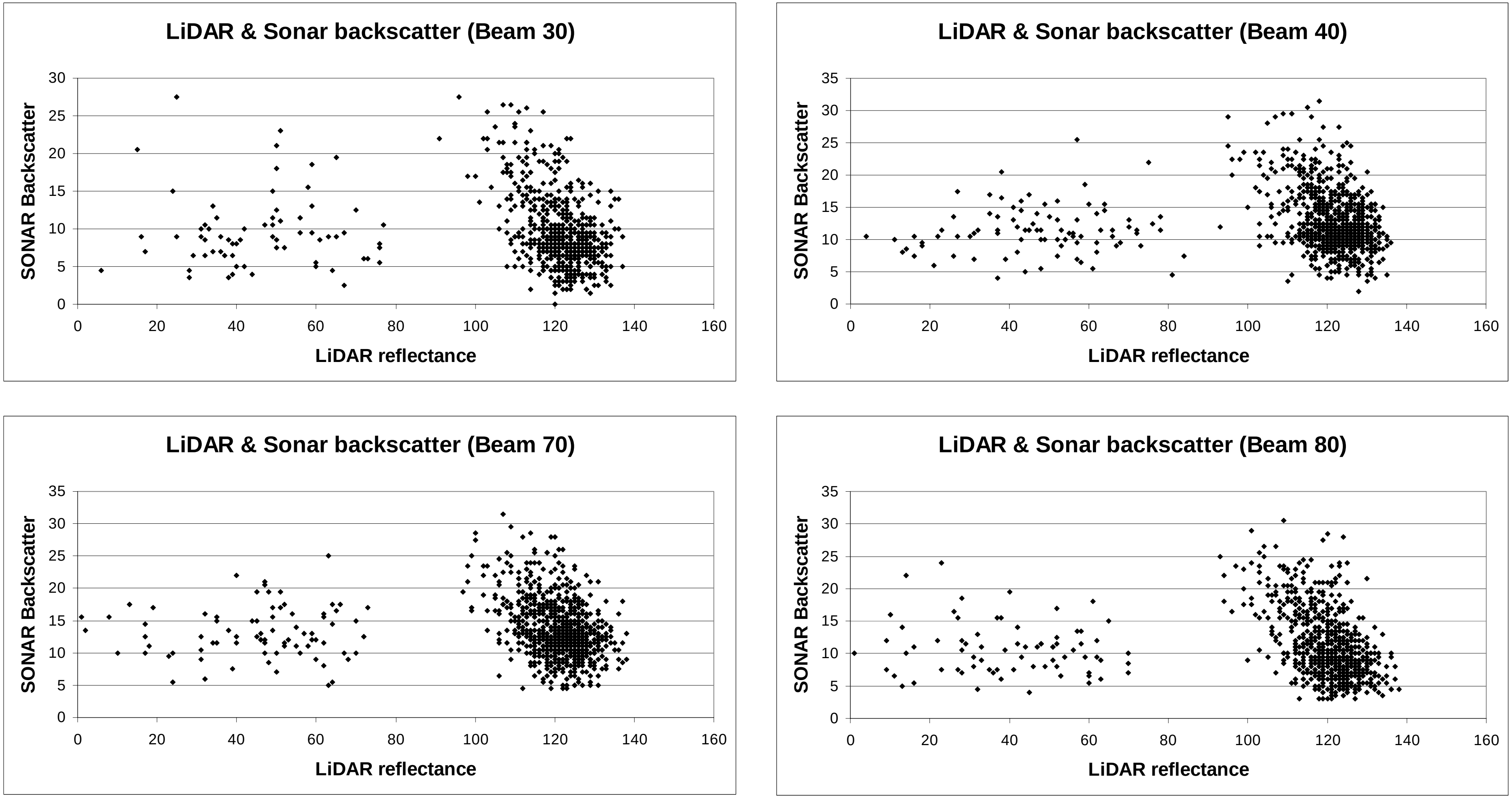

Figure 23: Scatter plot visualisation of global relationship between LiDAR reflectivity and MBES backscatter (for MBES beam numbers 30, 40, 70 and 80) for LiDAR MBES overlap area 2.

Statistical relationship tests

	Beam 30	Beam 40	Beam 70	Beam 80
Pearson’s Correlation	-0.13	-0.02	-0.07	-0.12
Pearson’s p-test	<0.001	<0.001	<0.001	<0.001
OLS regression	0.004			
Moran’s Index	0.03 (Clustered)			
Likelihood Moran’s-I result of random chance	<1%			

Table 12: Global and local statistical test results evaluating relationship between LiDAR reflectivity and MBES backscatter (for MBES beam numbers 30, 40, 70 and 80) for LiDAR MBES overlap area 2. *Note – OLS and Moran’s-I tests applied to entire overlap area 2.

Geographically Weighted Regression

LiDAR reflectivity and MBES backscatter for overlap area 2

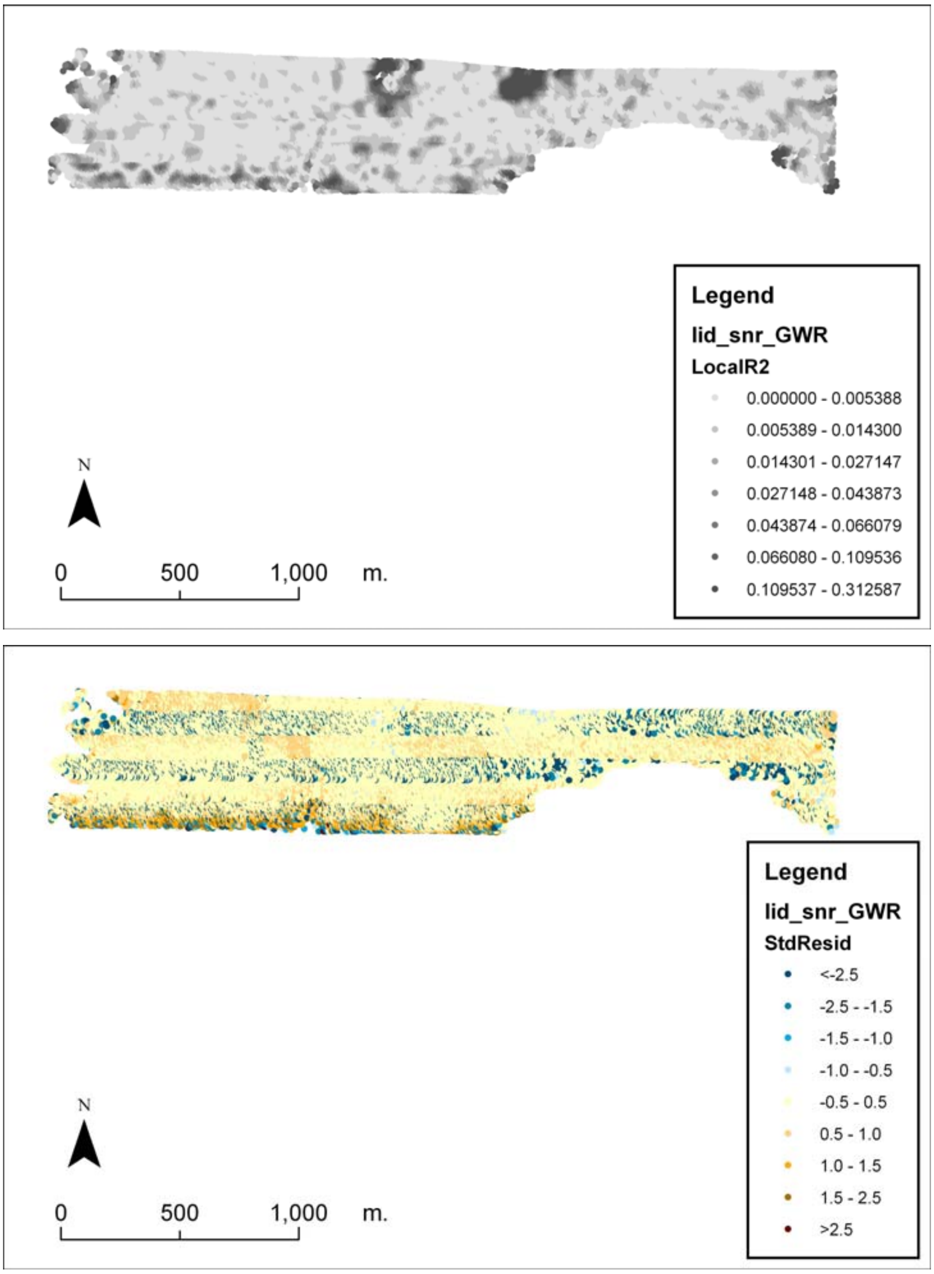

Figure 24: (a) local r^2 of local GWR, and (b) local standard residual of local GWR testing applied in Overlap area 2.

Overlap area 2: Summary of results

The results for overlap area 2 were similar to overlap area 1 in terms of the global measures, but displayed slightly more encouraging results in the local analysis. In terms of the global measures, the scatter plots (figure 23) Pearson's correlation and OLS regression results (table 12) all suggested a weak relationship between LiDAR reflectivity and MBES backscatter. The Moran's-Index value of 0.004 (table 12) suggested that a clustered pattern may be present, and the GWR local r2 values (figure 24a) while low, did suggest a relationship between LiDAR reflectivity and MBES backscatter in the shallower portions of overlap area 2. The range of depths in overlap area 2 was slightly wider, and included shallower depths than within overlap area 1. Local clustering patterns in the GWR local standard residuals map (figure 24a) appear to be related to similar values where successive LiDAR survey lines edge-lapped. Overall, these results suggested that water depth may have been too deep across the entirety of the overlap area 2, but evidence for a relationship in shallower areas was encouraging.

Shallow-water testing

The clear relationship observed (in section 3) between LiDAR reflectivity and depth strongly suggests that the relationship between LiDAR reflectivity and MBES backscatter requires further examination in shallow areas. LiDAR surveys conducted in Blacksod Bay during autumn 2010 will likely provide such an opportunity. This section will be updated in a revised version of this report after INFOMAR receives delivery of the autumn 2010 LiDAR data.

Flat area sub-tests in Overlap area 1

The comparative analyses of the relationship between LiDAR reflectivity and MBES backscatter that were conducted in overlap areas 1 and 2 failed to indicate a strong relationship between them. However, the issue of depth variability (i.e. lack of flatness) within some of the data (especially in overlap area 2) so additional tests were applied in relatively flat sections of overlap area 1 to see if stronger relationship between LiDAR reflectivity and MBES backscatter might be observed in flatter areas. Three sub-areas were selected, each encompassing relatively large and flat sub-sectors within overlap area 1. Sub-area 'A' was characterised by depths ranging from 19m – 21.5m, sub-area 'B' encompassed depths from 17m – 19m metres and sub-area 'C' covered depths from 20m – 22m metres.

Overlap area 1 - Flat area sub-tests

Subset areas and Scatter plot relationship visualisation

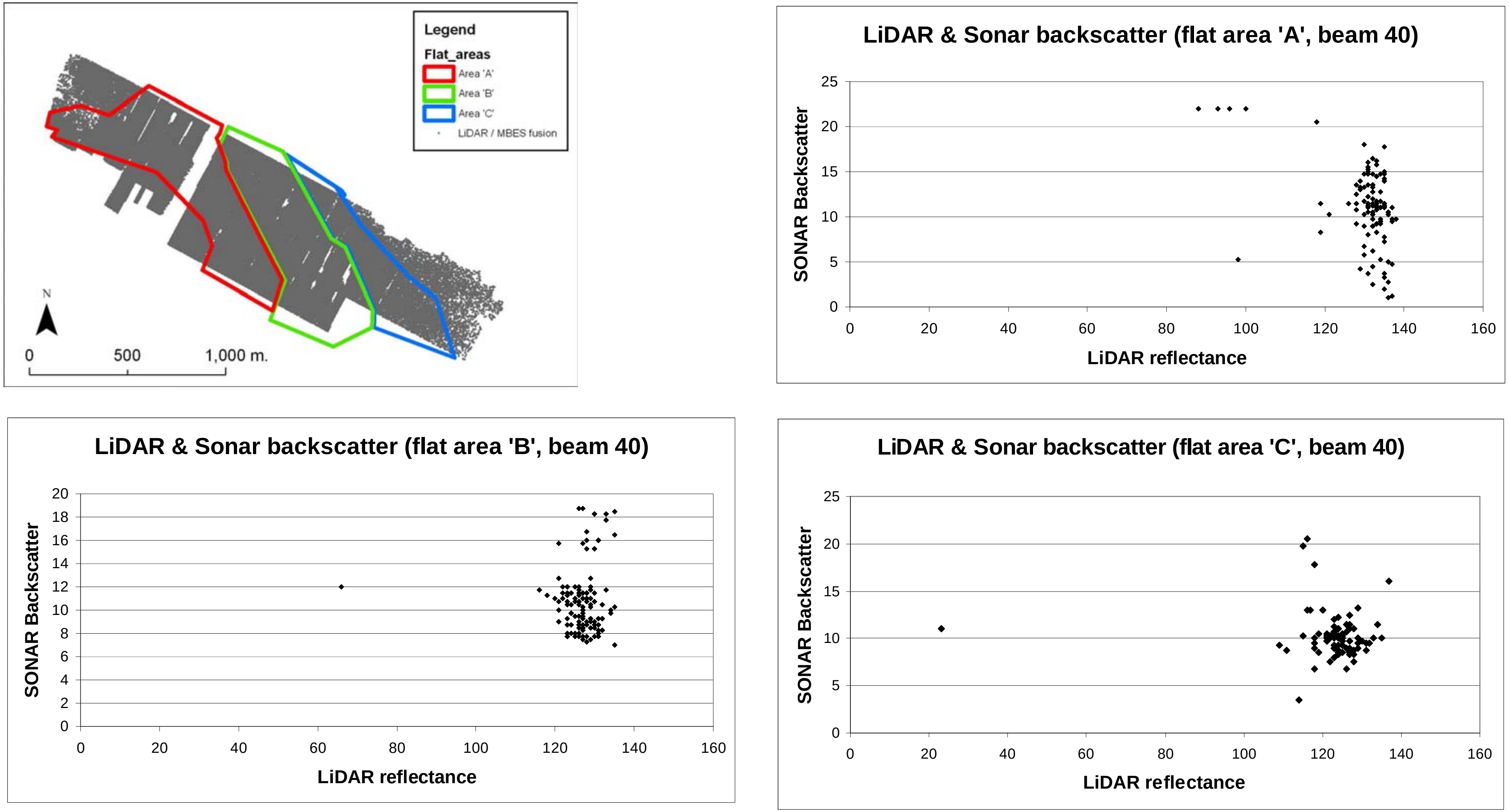

Figure 25: (a)'Flat' subset areas within Overlap area 1, (b) Scatter plot visualisation of global relationship between LiDAR reflectivity and MBES backscatter (for MBES beam number 40) in subset area 'A', (c) beam 40 in subset area B, and (d) beam 40 in subset area C.

Statistical relationship tests

	Subset 'A'	Subset 'B'	Subset 'C'
Depth range	19m – 21.5m	17m – 19m	20m – 22m
Points	134	131	86
Pearson's Correlation	0.040	0.040	-0.07
Pearson's p-test	<0.001	<0.001	<0.001
OLS regression	*0.0002		
Moran's Index	*0.038		
Likelihood Moran's-I result of random chance	<1%		

Table 13: Global and local statistical test results evaluating relationship between LiDAR reflectivity and MBES backscatter (for MBES beam number 40) within 'Flat' sub-areas A, B and C of Overlap area 1.

Flat area sub-tests – Summary of results

The results for the flat area sub-tests were very similar to the results for the whole of overlap area 1, indicating that sub-dividing the data into depth categories made no discernible difference in this location. The scatter plots (figure 25) Pearson's correlation and OLS regression results (table 13) all indicated a weak relationship between LiDAR reflectivity and MBES backscatter. No local statistical tests were applied because of the small number of points in each sub-area. Examining flat sub-areas separately may well be worthwhile in shallow water, but in this case it seems that the overall water depth was too deep.

Note:

Additional tests are required in shallower water in order to reach a reliable conclusion about the relationship between LiDAR reflectivity and MBES backscatter. These tests will be carried out after the 2010 LiDAR survey data have been delivered to INFOMAR and the content of this report will be updated accordingly.

Section 5 – Discussion

The study attempted to answer three main questions, namely:

1 What is the quality of the LIDAR reflectivity data in survey line overlap and non-overlap areas?

2 To what extent are LiDAR reflectivity values modified by depth, slope and LiDAR scan angle?

3 How does LiDAR reflectivity compare with sonar backscatter (and by extension can some conclusions be drawn from this study regarding the potential for LiDAR reflectivity to be used to map seabed character?)

With regard to question one, comparison of LiDAR reflectivity values in LIDAR survey line edge-lap and non edge-lap areas confirmed that reflectivity values were consistent in both. A tendency was observed for the larger number of data points in edge-lap areas to subtly influence some statistical analyses, but this was not related to data quality, and it did not affect the analysis.

In terms of question number two, the dependence of depth, seabed slope and scan angle on LiDAR reflectivity was confirmed. Depth was found to be by far the biggest influence on reflectivity, and this was found to be significant up to depths of approximately 15 metres. The relationship between LiDAR reflectivity and seabed slope was found to be important also (up to depths of about 15 metres) indicating its own dependence on depth. In terms of scan-angle, a modest relationship was observed between it and LiDAR reflectivity.

Question three was more difficult to answer, chiefly because of the depth of the areas where LIDAR / MBES overlaps were available. Unfortunately the majority of the overlap areas were at depths of 20 metres and more. Therefore, the apparent lack of evidence for a relationship between LiDAR reflectivity and MBES backscatter should be considered in this light. Furthermore, given the strong relationship observed earlier between depth and LiDAR reflectivity it seems probable that depth affected the test outcomes.

Recent LiDAR surveys conducted in the Blacksod bay area are expected to provide an opportunity to evaluate the relationship between LiDAR reflectivity and MBES backscatter in shallow water areas. It is anticipated that it will be possible to provide an updated version of this report after the relevant data are delivered to INFOMAR. In addition, recent publications (Chust et al. 2010, Costa et al. 2009) suggest that data issuing from newer bathymetric LiDAR systems may provide more scope for reflectivity-based seabed characterisation than older systems.

Section 6 – Possible future work required

Additional analysis in shallow-water areas would definitely be worth exploring, and can be done and supplied within an updated version of this report after the 2010 LiDAR data for Blacksod bay are delivered to INFOMAR. Reflectivity data captured using newer bathymetric LiDAR systems may also produce better results than can be expected from Tenix LADS data (Costa et al. 2009).

The affect of sea-surface reflectivity on lidar reflectivity has been found to be a significant factor affecting bathymetric LiDAR reflectivity (Chust et al. 2010). There may be scope to assess the affect of normalising lidar reflectance based upon visible spectrum reflectance on simultaneously-acquired imagery captured with LADS and Peregrine datasets and the scope for image data to be used in conjunction with LiDAR bathymetry and reflectivity data may also be worth exploring.

The apparently linear relationship observed in section three between LiDAR reflectivity and depth, and LiDAR reflectivity and slope suggests that there may be scope for further work assessing the potential for normalisation of existing LiDAR reflectivity datasets based upon depth and slope.

References

Chi-Kuei, W. and Philpot, W.D., 2007, Using airborne bathymetric LiDAR to detect bottom type variation in shallow waters, Remote Sensing of Environment 106, pp. 123–135.

Chust, G.,*, Grande, M., Galparsoro, I., Uriarte, A. and Borja, A., 2010, Capabilities of the bathymetric Hawk Eye LiDAR for coastal habitat mapping: A case study within a Basque estuary, Estuarine, Coastal and Shelf Science 89, pp. 200-213.

Costa, B.M., Battista, T.A., and Pittman, S.J., 2009, Comparative evaluation of airborne LiDAR and ship-based multibeam Sonar bathymetry and intensity for mapping coral reef ecosystems, Remote Sensing of Environment 113, pp. 1082–1100.

Coveney, S. and Monteys, X., (***In Press***), Integration Potential of INFOMAR Bathymetric LiDAR with External Onshore LiDAR Datasets. Journal of Coastal Research Special issue no. 62.

Coveney, S., (2009), Integration of INFOMAR Bathymetric LiDAR with external onshore LiDAR datasets, INFOMAR research report INF-08-06-COV.